AD_____

CONTRACT NUMBER: DAMD17-93-C-3040

TITLE: Protection Against the Acute and Delayed Toxicities of Sulfur Mustard

PRINCIPAL INVESTIGATOR: David B. Ludlum, Ph.D., M.D.

CONTRACTING ORGANIZATION: University of Massachusetts
Medical Center
Worcester, MA 01655

REPORT DATE: April 1996

TYPE OF REPORT: Final

PREPARED FOR: Commander
U.S. Army Medical Research and Materiel Command
Fort Detrick, Frederick, MD 21702-5012

DISTRIBUTION STATEMENT: Approved for public release;
distribution unlimited

The views, opinions and/or findings contained in this report are those of the author(s) and should not be construed as an official Department of the Army position, policy or decision unless so designated by other documentation.

REPORT DOCUMENTATION PAGE

Form Approved
OMB No. 0704-0188

1. AGENCY USE ONLY (Leave blank)	2. REPORT DATE	3. REPORT TYPE AND DATES COVERED
	April 1996	Final (4 Dec 92 - 3 Mar 96)

4. TITLE AND SUBTITLE
Protection Against the Acute and Delayed Toxicities of Sulfur Mustard

5. FUNDING NUMBERS
DAMD17-93-C-3040

6. AUTHOR(S)
David B. Ludlum, Ph.D., M.D.

7. PERFORMING ORGANIZATION NAME(S) AND ADDRESS(ES)
University of Massachusetts Medical Center
Worcester, MA 01655

8. PERFORMING ORGANIZATION REPORT NUMBER

9. SPONSORING/MONITORING AGENCY NAME(S) AND ADDRESS(ES)
U.S. Army Medical Research and Materiel Command,
Fort Detrick, Frederick, MD 21702-5012

10. SPONSORING/MONITORING AGENCY REPORT NUMBER

11. SUPPLEMENTARY NOTES

12a. DISTRIBUTION/AVAILABILITY STATEMENT
Approved for public release;
distribution unlimited

12b. DISTRIBUTION CODE

13. ABSTRACT *(Maximum 200 words)*

Based on the chemotherapeutic literature and cell culture studies of sulfur mustard (SM) toxicity reported here, we believe that DNA repair mechanisms act as cellular defenses against SM toxicity. Cell culture studies show that survival is increased by the nucleotide excision repair mechanism while biochemical studies show that human as well as bacterial glycosylase enzymes can release two SM-induced DNA adducts: 7-hydroxyethylthioethyl guanine and 3-hydroxyethylthioethyl adenine. The growth of cultured human fibroblasts exposed to 10 μM SM appears to be enhanced in comparison with cells incubated continuously at 37°C by subjecting them to a period of hypothermia at 28°C before returning them to 37°C incubation. Cells held at 28°C undergo cell cycle arrest and we believe that this arrest may allow more time for DNA repair before the next round of cell division, thus enhancing survival. Concurrently, we have developed a ^{32}P-postlabeling method that can detect one 7-hydroxyethylthioethyl guanine in 10^6 DNA nucleotides in DNA extracted from SM-exposed cells. This method should prove useful in both exposure and DNA repair studies.

14. SUBJECT TERMS	15. NUMBER OF PAGES
Sulfur mustard, DNA damage, DNA repair, nucleotide excision repair, glycosylase, DNA adducts, cell cycle progression, cell cycle arrest, hypothermia, ^{32}P-postlabeling analysis.	54
	16. PRICE CODE

17. SECURITY CLASSIFICATION OF REPORT	18. SECURITY CLASSIFICATION OF THIS PAGE	19. SECURITY CLASSIFICATION OF ABSTRACT	20. LIMITATION OF ABSTRACT
Unclassified	Unclassified	Unclassified	Unlimited

GENERAL INSTRUCTIONS FOR COMPLETING SF 298

The Report Documentation Page (RDP) is used in announcing and cataloging reports. It is important that this information be consistent with the rest of the report, particularly the cover and title page. Instructions for filling in each block of the form follow. It is important to ***stay within the lines*** to meet ***optical scanning requirements***.

Block 1. Agency Use Only *(Leave blank)*.

Block 2. Report Date. Full publication date including day, month, and year, if available (e.g. 1 Jan 88). Must cite at least the year.

Block 3. Type of Report and Dates Covered. State whether report is interim, final, etc. If applicable, enter inclusive report dates (e.g. 10 Jun 87 - 30 Jun 88).

Block 4. Title and Subtitle. A title is taken from the part of the report that provides the most meaningful and complete information. When a report is prepared in more than one volume, repeat the primary title, add volume number, and include subtitle for the specific volume. On classified documents enter the title classification in parentheses.

Block 5. Funding Numbers. To include contract and grant numbers; may include program element number(s), project number(s), task number(s), and work unit number(s). Use the following labels:

C	- Contract	**PR**	- Project
G	- Grant	**TA**	- Task
PE	- Program Element	**WU**	- Work Unit Accession No.

Block 6. Author(s). Name(s) of person(s) responsible for writing the report, performing the research, or credited with the content of the report. If editor or compiler, this should follow the name(s).

Block 7. Performing Organization Name(s) and Address(es). Self-explanatory.

Block 8. Performing Organization Report Number. Enter the unique alphanumeric report number(s) assigned by the organization performing the report.

Block 9. Sponsoring/Monitoring Agency Name(s) and Address(es). Self-explanatory.

Block 10. Sponsoring/Monitoring Agency Report Number. *(If known)*

Block 11. Supplementary Notes. Enter information not included elsewhere such as: Prepared in cooperation with...; Trans. of...; To be published in.... When a report is revised, include a statement whether the new report supersedes or supplements the older report.

Block 12a. Distribution/Availability Statement. Denotes public availability or limitations. Cite any availability to the public. Enter additional limitations or special markings in all capitals (e.g. NOFORN, REL, ITAR).

- **DOD** - See DoDD 5230.24, "Distribution Statements on Technical Documents."
- **DOE** - See authorities.
- **NASA** - See Handbook NHB 2200.2.
- **NTIS** - Leave blank.

Block 12b. Distribution Code.

- **DOD** - Leave blank.
- **DOE** - Enter DOE distribution categories from the Standard Distribution for Unclassified Scientific and Technical Reports.
- **NASA** - Leave blank.
- **NTIS** - Leave blank.

Block 13. Abstract. Include a brief *(Maximum 200 words)* factual summary of the most significant information contained in the report.

Block 14. Subject Terms. Keywords or phrases identifying major subjects in the report.

Block 15. Number of Pages. Enter the total number of pages.

Block 16. Price Code. Enter appropriate price code *(NTIS only)*.

Blocks 17. - 19. Security Classifications. Self-explanatory. Enter U.S. Security Classification in accordance with U.S. Security Regulations (i.e., UNCLASSIFIED). If form contains classified information, stamp classification on the top and bottom of the page.

Block 20. Limitation of Abstract. This block must be completed to assign a limitation to the abstract. Enter either UL (unlimited) or SAR (same as report). An entry in this block is necessary if the abstract is to be limited. If blank, the abstract is assumed to be unlimited.

★U.S.GPO:1991-0-299-935

FOREWORD

Opinions, interpretations, conclusions and recommendations are those of the author and are not necessarily endorsed by the US Army.

N/A Where copyrighted material is quoted, permission has been obtained to use such material.

N/A Where material from documents designated for limited distribution is quoted, permission has been obtained to use the material.

N/A Citations of commercial organizations and trade names in this report do not constitute an official Department of Army endorsement or approval of the products or services of these organizations.

N/A In conducting research using animals, the investigator(s) adhered to the "Guide for the Care and Use of Laboratory Animals," prepared by the Committee on Care and Use of Laboratory Animals of the Institute of Laboratory Resources, National Research Council (NIH Publication No. 86-23, Revised 1985).

N/A For the protection of human subjects, the investigator(s) adhered to policies of applicable Federal Law 45 CFR 46.

N/A In conducting research utilizing recombinant DNA technology, the investigator(s) adhered to current guidelines promulgated by the National Institutes of Health.

N/A In the conduct of research utilizing recombinant DNA, the investigator(s) adhered to the NIH Guidelines for Research Involving Recombinant DNA Molecules.

N/A In the conduct of research involving hazardous organisms, the investigator(s) adhered to the CDC-NIH Guide for Biosafety in Microbiological and Biomedical Laboratories.

Award B Cullum 3 Apr 96

PI - Signature Date

TABLE OF CONTENTS

page

INTRODUCTION

Background

Sulfur mustard (SM) was introduced as a chemical warfare agent in World War I. Although it was not employed in World War II, it has been used in several smaller conflicts since that time and is of concern as a possible terrorist weapon (1). Exposure to SM can cause serious injury to the skin, respiratory tract, and other mucous membranes (1), and the compound is considered carcinogenic by the International Agency for Research on Cancer (2); no effective antidote is yet available. The studies reported here are intended to elucidate the mechanism of toxicity and to develop methods of ameliorating it.

Early investigators showed that SM reacts with DNA, and it is generally believed that DNA modification initiates SM toxicity (3). When it was discovered that the closely-related nitrogen mustards have antitumor activity that is also based on DNA modification, these agents began to be used in cancer chemotherapy (4). In the ensuing years, there have been numerous investigations of other antitumor agents that act by modifying DNA (5-8). As a result, considerable information has accumulated about the nature of the DNA modifications produced by antitumor agents and about the ability of cells to protect themselves from this damage.

Perhaps surprisingly, DNA damaging agents are also found in nature. An important cellular metabolite, S-adenosylmethionine, is actually a one-armed sulfur mustard that can alkylate DNA (9,10). Consequently, cells have developed defenses against the kinds of DNA damage inflicted by SM and other alkylating agents. A major objective of our work is to enhance these natural defenses.

Overall, we are investigating the hypotheses that (a) DNA damage is the initiating event in sulfur mustard toxicity, (b) repair of this damage by cellular enzymes can reduce cytotoxicity, and (c) alteration of the cell cycle by physical or chemical means may allow increased time for repair and lead to decreased cytotoxicity.

In this Introduction, we will review briefly what is known about the DNA damage that is caused by SM and consider methods of measuring levels of SM-induced DNA adducts. Evidence for repair of SM-induced DNA damage will also be reviewed. Finally, methods for modulating cell cycle progression in order to allow time for increased DNA repair will be considered. The bulk of this report summarizes our progress in the three areas mentioned in the paragraph above.

Sulfur Mustard-induced DNA Modifications

As reported originally by Brooks and Lawley (11), the principal adduct formed in DNA by SM is 7-hydroxyethylthioethyl guanine (HETEG), which accounts for approximately 60% of the total alkylation. This finding has been confirmed on numerous occasions, most recently by Benschop *et al.* (12) and by our laboratory (13). Smaller amounts of 3-hydroxyethylthioethyl adenine (HETEA) and the cross-link, di-(2-guanin-7-yl-ethyl)sulfide, have also been found consistently.

Studies of chemotherapeutic agents have shown that DNA modifications which are present in relatively small amounts may nevertheless be the primary cause of cytotoxicity. Of particular importance is alkylation at the O^6-position of guanine (8). Accordingly, minor modifications cannot be dismissed as unimportant, and several of these have been identified in reactions of the one-armed mustard, chloroethylethyl sulfide, with DNA (14,15). Similar minor products are probably formed by SM as well, but attempts to identify O^6-hydroxyethylthioethyl guanine (O^6-HETEG) in DNA that has been reacted with SM have been unavailing (16).

For the purposes of evaluating exposure, we and other investigators have focused on the most abundant DNA modification. Antibodies that recognize HETEG have been developed and used successfully to measure levels of DNA damage in cells exposed to SM (12). We report here the successful use of the ^{32}P-postlabeling method to detect HETEG in fibroblasts exposed to SM. This methodology should prove useful in evaluating methods of protecting cells against SM and of minimizing the consequences of exposure.

Repair of SM-induced DNA Modifications

Since alkylating agents occur in nature, it is not surprising that cells have developed defenses against such agents. Intracellular material, particularly glutathione, can combine with alkylating agents and prevent their reactions with DNA. Once reaction with DNA has occurred, however, the cell still has the ability to repair this damage.

Early investigators obtained evidence for the enzymatic removal of the adducts from the DNA of *E. coli* exposed to low levels of SM (17-19). Subsequently, other investigators have shown that adducts are also removed from the DNA of mammalian cells exposed to SM (20-22).

Papirmeister *et al.* (23) found that bacterial extracts catalyzed the release of 3-substituted adenines produced in DNA by 2-chloroethyl-2-hydroxyethyl sulfide (hemisulfur mustard) and attributed this release to the presence of a glycosylase. Glycosylase action results in the formation of apurinic sites which are subject to endonuclease action and subsequent repair. Although the extracts tested by Papirmeister *et al.* (23) were inactive in releasing the 7-substituted guanine formed by hemisulfur mustard, Habraken *et al.* (24) showed that bacterial 3-methyladenine DNA glycosylase II releases two monoadducts formed by chloroethylethyl sulfide (CEES), 3-ethylthioethyl adenine and 7-ethylthioethyl guanine. In fact, activity towards these bases was comparable to activity towards methylated bases.

When [^{14}C]-labeled SM of sufficiently high specific activity became available to us under this contract, we were able to test the activity of bacterial 3-methyladenine DNA glycosylase II towards the adducts produced in DNA by SM itself. As reported below, this enzyme has similar activity towards the hydroxyethylthioethyl-substituted guanine and adenine formed by SM as it has towards the ethylthioethyl derivatives formed by CEES.

Recently, a plasmid bearing the cloned human gene for glycosylase has become available to us through the courtesy of Professor Leona Samson of Harvard University, and we have made substantial progress in purifying human glycosylase.

As reported below, the human enzyme as well as the bacterial enzyme has activity towards the 7-hydroxyethylthioethyl guanine and 3-hydroxyethylthioethyl adenine introduced into DNA by SM. However, neither enzyme appears to release the cross-link, di-(2-guanin-7-yl-ethyl)sulfide, from DNA.

In summary, the protective action of DNA repair mechanisms has been established, and details of the process are currently being investigated. It seems likely that efforts to increase the efficiency of repair will decrease SM toxicity.

Protection against SM-induced Cytotoxicity

The toxicity of micromolar concentrations of SM is easily demonstrated in cell culture. As might be expected, however, different cell lines exhibit different levels of sensitivity to SM, and differences among the cell lines need to be taken into account in interpreting cytotoxicity data. Whether or not cell cycle regulatory mechanisms are intact is particularly relevant to the hypothesis that a delay in cell cycle progression may allow time for increased DNA repair.

Important background information on cell cycle progression is becoming available from studies of cancer chemotherapy. In that area, if a cell cannot arrest its cell cycle progression to allow time for more DNA repair, the cytotoxicity of a DNA modifying antitumor agent may be increased, and this may lead to a desirable increase in therapeutic response. Cell cycle progression as it relates to chemotherapy has been reviewed recently with a particular emphasis on the role of p53 whose function appears to be required for cell cycle arrest (25-30).

Since the ability to arrest the cell cycle and allow time for repair is important to our hypothesis, we have chosen to study nontumorigenic cell lines in which cell cycle regulatory mechanisms are probably intact. Thus, we have investigated normal human fibroblasts and a human keratinocyte line obtained from Dr. Howard P. Baden's laboratory at the Massachusetts General Hospital. In addition, we have investigated Chinese hamster ovary (CHO) cells which have the advantage that mutants in DNA excision repair have been characterized.

Both chemical and physical methods are available for slowing the progression of cells through their replicative cycle and the application of these modalities may allow time for more effective DNA repair. For example, the agent, ciclopirox olamine (CPX), causes a G_1/S arrest which is reversible when the agent is removed (31,32). If DNA repair continues in the presence of CPX, survival might be increased after a period of recovery under CPX treatment.

Data included in this report show that a period of hypothermia causes a generalized cell cycle arrest which apparently improves recovery of cell growth under certain conditions. Hypothermia probably slows all metabolic processes including repair, but repair of radiation-induced DNA damage has been shown to be increased by a period of hypothermia (33,34). Conversely, hyperthermia increases cell damage by cancer chemotherapeutic agents (35). Thus, we believe that it will be possible to find hypothermic conditions under which DNA repair can be enhanced by modulating cell cycle progression.

MATERIALS AND METHODS

Materials

Reagents

[^{14}C]SM, uniformly labeled in the chloroethyl group, as well as unlabeled SM, were supplied by the Analytical Chemistry Branch, U.S. Army Medical Research Institute of Chemical Defense. Two batches of [^{14}C]SM were received which had different specific activities (SA): 30 May 90 batch, SA = 0.88 mCi/mmol and 22 Mar 95 batch, SA = 64.5 mCi/mmol. 2-Chloroethyl-2-hydroxyethyl sulfide (hemisulfur mustard, HSM) was prepared by reacting 2-mercaptoethanol with 1,2-dichloroethane according to Tsou *et al* (36) as described previously (37). 6-Chloro-2-amino purine deoxyriboside was a gift of Prof. George Wright, University of Massachusetts (38). Mercaptoethanol, ciclopirox olamine (CPX), MTT (dimethylthiazolyl-diphenyltetrazolium), micrococcal nuclease, P1 nuclease, proteinase K, calf thymus DNA and all nucleosides and nucleotides were purchased from Sigma. 1-Iodobutane, triethylamine, 1,2-dichloroethane, sodium hydride, 6-chloro-2-amino purine, and bis-hydroxyethyl sulfide were obtained from Aldrich; spleen phosphodiesterase, from Worthington Biochemical Corporation; and T4 polynucleotide kinase, from New England Biolabs. [γ-^{32}P]ATP (3000 Ci/mmol) was purchased from New England Nuclear. DEAE Sephadex A-25 anion exchange resin (capacity, 3.5 meq/g; particle size, 40-120μ) was obtained from Pharmacia. Serum-free media (SFM) for the growth of keratinocytes was obtained from Gibco. Chromatography-grade solvents, media ingredients, and other reagents were obtained from standard sources.

A plasmid bearing cloned *E. coli* 3-methyladenine DNA glycosylase II was supplied by Prof. Mutsuo Sekiguchi of Kyoto University in Japan. A plasmid containing the cloned gene for human 3-methyladenine DNA glycosylase was obtained from Prof. Leona Samson, Harvard School of Public Health, Boston, MA. Methylated DNA substrate for assaying these enzymes was prepared by our published procedure (39).

Cell Lines

Human fibroblasts (AG1522B) were obtained from the Coriell Cell Repository and human keratinocytes (NM-1 cells) were obtained from Dr. Howard P. Baden's laboratory, Massachusetts General Hospital, Charlestown, MA. Established Chinese hamster ovary (CHO) cell lines that are competent (AA8, wild type) or deficient (UV41) in nucleotide excision repair were obtained from the American Type Culture Collection. Neither CHO line has detectable O^6-alkylguanine-DNA alkyltransferase activity (40); in order to determine the effect of O^6-alkylguanine-DNA alkyltransferase, CHO cells transfected with a plasmid expressing human O^6-alkylguanine-DNA alkyltransferase were obtained from Dr. E. Bresnick of this institution (41).

Methods

Synthesis of HPLC Markers

It is essential to have standard SM-modified nucleotides available in

the ^{32}P-postlabeling technique to establish labeling conditions and HPLC retention times. 7-Hydroxyethylthioethyldeoxyguanosine 3'-phosphate (HETEdGp) was synthesized as described previously (37). Briefly, HSM (30 μl, 0.21 mmol) was reacted with 2'-deoxyguanosine 3'-phosphate (dGp, 10 mg, 0.029 mmol) in 1 ml of 100 mM KH_2PO_4 buffer, pH 3.5, for 2 h at room temperature. The pH was adjusted to 7 and the reaction mixture was separated, 0.5 ml at a time, on an A-25 anion exchange column (1 x 10 cm) eluted with 60 mM triethylammonium acetate (TEAA), pH 7.0, at a flow rate of 0.8 ml/min; purification was performed in a cold cabinet to minimize depurination. Twenty min fractions were collected and the major product appeared in fractions 4 to 6. This product had the same UV spectrum as HETEdGp, and released HETEG on depurination. 7-Hydroxyethylthioethyldeoxyguanosine 5'-phosphate (HETEpdG) was produced by the corresponding reaction with pdG.

7-Butyldeoxyguanosine 3'-phosphate (BudGp) and 7-butyldeoxyguanosine 5'-phosphate (BupdG) for use in the internal standardization procedure were synthesized by reacting n-butyliodide in DMSO with the triethylammonium salts of dGp and pdG, respectively. These nucleotides, purified as for HETEdGp and HETEpdG, depurinated to 7-butylguanine; the structure of this base was established by its characteristic ultraviolet spectra in acid, neutral, and basic pH, and its molecular weight of 207 obtained by fast atom bombardment mass spectrometry. Fast atom bombardment mass spectrometry was performed for us by Mr. Marion Kirk at the University of Alabama in Birmingham, AL.

O^6-hydroxyethylthioethyl deoxyguanosine, the expected product of O^6-deoxyguanosine alkylation by SM, was synthesized from 6-chloro-2-amino purine deoxyriboside by displacement of the chlorine atom. Sodium hydride (100 mg, 60% dispersed in mineral oil, 2.5 mmol) was added slowly with stirring to bis-hydroxyethylsulfide (2 ml, 20 mmol) in a 3-necked flask under nitrogen. Then, 6-chloro-2-amino purine deoxyriboside (5 mg, 0.02 mmol) dissolved in 0.5 ml dried DMF was added dropwise and the mixture was stirred overnight at 37°C. The reaction mixture was neutralized with dilute formic acid and purified by passage through a G-10 column (2.5 x 100 cm) eluted at 0.7 ml/min with 1 mM formic acid. The ultraviolet absorbance of the eluent was monitored and 30 min fractions were collected. The product appeared in fractions 35-42 which were pooled and lyophilized to recover O^6-hydroxyethylthioethyl deoxyguanosine with a 75% yield. The structure of the product was established by its characteristic ultraviolet spectrum and its molecular weight of 371 obtained by mass spectrometry, in agreement with data published by Fidder *et al.* (16). O^6-hydroxyethylthioethyl guanine was synthesized by a similar displacement of chlorine from 6-chloro-2-amino purine.

The HPLC marker for the SM-induced cross-link, di-(2-guanin-7-yl-ethyl)sulfide, was kindly supplied by Dr. H. P. Benschop, TNO-Prins Maurits Laboratory, The Netherlands.

Preparation of [^{14}C]SM-modified DNAs

To prepare a radiolabeled SM-modified DNA for calibration of the ^{32}P-postlabeling method, DNA was modified with low SA [^{14}C]SM to provide DNAs with known HETEG content. [^{14}C]SM (1 mg/ml in toluene, 0.88 mCi/mmol) was added to 10 ml calf thymus DNA (6 mg/ml) in 50 mM of sodium cacodylate buffer, pH 7.0, to bring the final concentration of SM to approximately 200 μM. After incuba-

tion with continuous mixing for 2 h at 37°C, 1/20th volume of 6 N NaCl and two volumes of 95% ethanol were added to precipitate the DNA; the precipitate was washed free of noncovalently bound material by repeated dissolutions and reprecipitations from buffer solution. The level of HETEG in this sample was determined from the optical density and HETEG content of an aliquot to be 630 HETEG/10^6 DNA nucleotides. HETEG content was determined by depurinating the sample and measuring the radioactivity of the HETEG peak in an HPLC separation as described previously (13,37). A solution of unmodified DNA was blended with a solution of this sample to obtain DNAs ranging in HETEG content down to 0.087 HETEpdG/10^6 DNA nucleotides.

To prepare a radiolabeled substrate suitable for glycosylase studies, calf thymus DNA was modified with the higher SA batch of [^{14}C]SM. The reaction of [^{14}C]SM with DNA, purification, and characterization of the substrate were carried out as described above. However, since the modified bases in this DNA have the same high SA as the original [^{14}C]SM (i.e. 64.5 mCi/mmol), they are sufficiently radioactive to be detected in a standard glycosylase assay. The composition of this substrate as well as the composition of the [^{3}H]DMS-modified DNA used in comparison experiments is given in the Results Section.

^{32}P-Postlabeling Method for Detecting SM Damage to DNA

This stepwise procedure, slightly modified after Yu *et al.* (42), is shown in the flow diagram on the next page (Figure 1). ^{32}P-postlabeling is dependent on the successful digestion of DNA into its constituent deoxynucleotide 3'-phosphates as a first step because a 3'-phosphate is required for labeling; the labeling enzyme (T4 kinase) adds a 5'-phosphate to a substrate only when a 3'-phosphate is present. A critical step in the successful application of the ^{32}P-postlabeling method to SM-modified DNA was the discovery that low temperature digestion was possible and that it preserved the unstable HETEdGp. Another critical step in obtaining accurate analyses was the inclusion of an internal standard of BudGp from the beginning of the analysis. Since this nucleotide has chromatographic and stability characteristics similar to those of HETEdGp, it can be used to correct for physical losses and decomposition of HETEdGp. Furthermore, since amounts of HETEpdG are determined by a ratio to the internal standard, it is not necessary to know the specific activity of the [^{32}P]ATP accurately to calculate the HETEpdG content.

A detailed explanation of each step of the ^{32}P-postlabeling technique as it is applied to SM-modified DNA follows.

DNA was digested into its constituent 3'-nucleotides by two enzymes: micrococcal nuclease (an endonuclease that cleaves phosphodiester bonds to leave 3'-phosphates) and spleen phosphodiesterase (an exonuclease that releases 3'-mononucleotides). Typically, 50 μg of DNA was digested overnight at 10°C in 160 μl containing 0.3 M triethylammonium acetate buffer, pH 7.5; 5 mM $CaCl_2$; 0.3 unit spleen phosphodiesterase and 6 units micrococcal nuclease.

We have found that HETEdGp is depurinated if this hydrolysis reaction is performed at the usual temperature, 37°C. However, if the digestion is performed at 10°C, approximately 50% of the derivative is released as the 3'-mononucleotide and is, therefore, capable of being phosphorylated by the T4 enzyme.

Since the normal nucleotides greatly exceed the derivative nucleotides in number, perhaps by 10^7 to 1, it is desirable to remove these before the ^{32}P-postlabeling step. N-7-substituted guanine nucleotides are separated efficiently from normal nucleotides on an anion exchange column because they bear a positive charge at the N-7 position (43,44). We have found it convenient to perform both the initial separation of the nucleotides in the enzymatic digest and the later separation of labeled N-7 adducts from [^{32}P]ATP on disposable columns. These are made by packing 1 ml plastic tuberculin syringes with 1 ml of A-25 resin pre-equilibrated in 0.2 M TEAA buffer, pH 7.0, to form columns measuring 4 x 68 mm. The columns are attached in an easily removable way to a Milton Roy pump through a plastic connector inserted into the syringe barrel, and to a UV monitor through a modified #17 needle. In the initial separation of N-7 adducts from normal nucleotides, an optical marker of BupdG was added; in the separation of labeled adducts from [^{32}P]ATP, an optical marker of HETEpdG was added. The column was eluted with 80 mM TEAA, pH 7.0, at a flow rate of 1 ml/min in both separations; in the initial separation involving unstable HETEdGp, cold buffer was used. Fractions containing N-7 guanine nucleotides, identified by the BupdG marker, were frozen immediately and lyophilized to dryness.

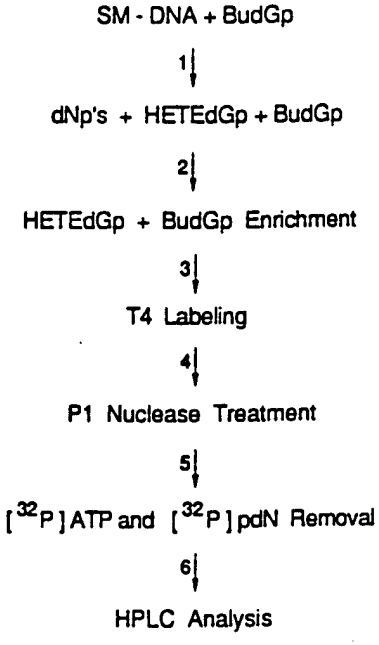

Figure 1. ^{32}P-Postlabeling Method for Detecting SM Damage to DNA. A known amount of BudGp determined spectrophotometrically (ϵ_{256} = 9800 at pH 7) is added as internal standard to an amount of DNA calculated from its A_{260} value (ϵ_{260} = 6800 at pH 7), and enzymatic digestion is carried out at 10°C (step 1). HETEdGp and BudGp separated quickly from unmodified nucleotides on a small column to minimize decomposition in step (2), and the solution is concentrated by lyophilization. In step (3), a ^{32}P label is added to the nucleotide 5′ position by T4 kinase. 3′-Phosphates are removed by P1 nuclease in step (4), and the labeled HETEpdG and BupdG are recovered from a disposable anion column in step (5). Residual radioactivity is discarded with the column at this point, minimizing laboratory handling of ^{32}P. Finally, HETEpdG and BupdG are separated from contaminating radioactivity by HPLC in step (6), and the amount of HETEpdG is calculated from the ratio of HETEpdG to BupdG radioactivity.

For levels of modification exceeding one HETEpdG/10^6DNA nucleotide, N-7 guanine nucleotides collected from 1 nmol (0.3 μg) of digested SM-DNA containing 2 fmol of BudGp were labeled in 5 μl of 0.14 M Tris-acetate buffer, pH 7.5, containing 28 mM $MgCl_2$, 28 mM dithiothreitol, 2.8 mM EDTA, and 2 mM spermidine. One μl of ATP (0.023 mM) and 5 μl of [^{32}P]ATP (50 μCi) were added, and the substrate was incubated with twenty units of T4 kinase for 90 min at 37°C. Then, 2 μl of 2 mM $ZnCl_2$ and two units of P1 nuclease were added and the incubation was continued for 1 h at 37°C to remove 3'-phosphates. For levels below one HETEpdG/10^6 DNA nucleotides, N-7 guanine nucleotides from as much as 40 nmol of DNA digest (13 μg) were labeled.

The labeling solution was mixed with an optical marker of HETEpdG and loaded onto a disposable A-25 column eluted at 1 ml/min with 80 mM TEAA buffer, pH 7.0. About 10 ml of buffer containing the HETEpdG optical peak were collected and lyophilized to dryness. Most of the [^{32}P]ATP remained on the column and was discarded in the radioactive waste.

The final HPLC analysis was performed on a modular apparatus consisting of a Milton Roy minipump, Rheodyne 7125 injection valve, and a 5 μm Spherisorb (4.6 x 250 mm) C_{18} column from Alltech. Elution profiles were monitored at 254 nm with a Perkin-Elmer LC-55B spectrophotometric detector interfaced with a Hewlett-Packard 3396A integrator. The column was eluted at 1 ml/min with 1% acetonitrile in 70 mM TEAA, pH 7.0, for 40 min; then with a gradient of 1 to 3% acetonitrile in TEAA from 40 to 70 min, and finally with 3% acetonitrile in TEAA from 70 to 84 min. One ml fractions were collected and the Cherenkov radiation in each fraction was determined in a scintillation counter. Radioactivity in individual peaks was automatically totaled by a computer program which subtracts background radiation.

Isolation of DNA from cultured cells

Some difficulties were encountered initially in applying the ^{32}P-postlabeling technique to DNA isolated from cultured cells. Literature procedures start with a cell lysis step followed by a RNAse step to remove RNA and a proteinase step to digest protein. Partially digested protein and proteinase itself is then usually removed with an organic extraction step which may involve the use of phenol or a mixture of chloroform and isoamyl alcohol. However, this approach led to irreproducible results when we applied it to the analysis of DNA isolated from cultured cells exposed to SM. This irreproducibility was traced to the use of organic solvents; when a blend with a known HETEpdG content was subjected to the organic extraction step, its HETEpdG content was drastically lowered. We assume that the fat soluble hydroxyethylthioethyl adducts are somehow removed from the DNA by the organic solvents. As an alternative to organic extraction, we utilized the salt precipitation method of Miller *et al.* to remove proteins (45).

Our current isolation procedure is shown in Figure 2 (next page). DNA was isolated from cultured cells which had been stored frozen in PBS, a treatment which probably facilitates lysis. Cells were warmed to room temperature, collected by centrifugation for 10 min at 1500 x g, suspended in 1 ml of 0.2 M Tris-HCl, pH 8.0, containing 0.05 M NaEDTA and 1% sodium dodecyl sulfate, and incubated with 250 μg of RNAse for 2 h at 37°C. Then, 400 μg of proteinase K was added and incubation was continued for an additional 2 h at 37°C. To re-

move protein, one ml of 6 M ammonium acetate was added, and precipitated protein was removed by centrifugation for 10 min at 7,000 x g in the cold. The supernatant was withdrawn, two volumes of cold ethanol were added, and the solution was cooled in a dry ice bath. Precipitated DNA was redissolved in 300 μl of water adjusted to pH 7.5, and concentration was determined from the ultraviolet scan of a diluted aliquot in a microcuvette. The ratio of optical absorbance at 260 nm to that at 280 nm averaged 1.85 ± .03; approximately 225 μg of DNA was recovered from 10^7 cells.

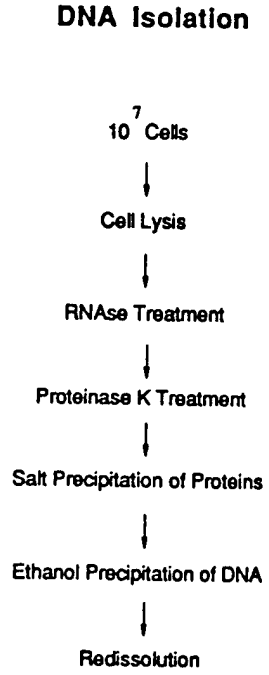

Figure 2. Method for Isolating DNA from Cultured Cells.

Purification of Glycosylase Enzymes

Bacterial 3-methyladenine DNA glycosylase II (Gly II) was purified from an overproducing strain of *E. coli* kindly provided by Professor Mutsuo Sekiguchi (46). Purification was performed according to Nakabeppu *et al.* (46) through the DNA-cellulose column step as described previously (24). The purified enzyme migrated as a single band on a 12.5% polyacrylamide-0.1% SDS gel at a molecular weight of 31,000. The enzyme was tested for nuclease activity against a double-stranded [^{3}H]thymidine DNA and the same DNA which contained apurinic sites. Negligible amounts of radioactivity were released into the ethanol-soluble fraction by the purified enzyme indicating that it was essentially free from non-specific nucleases. However, as a further precaution against nuclease activity, EDTA was added to incubations with [^{3}H]DMS-DNA and [^{14}C]SM-DNA.

Human 3-methyladenine DNA glycosylase was purified from a plasmid containing the cloned gene (pP5-3, ref 47) grown in *E. coli* (*alkA tag*) cells which do not contain any endogenous glycosylase activity. Cells (3.5 gm) grown to early log phase were homogenized in 60 ml of 20 mM Tris-HCl, pH 7.5, buffer containing 1

mM EDTA, 1 mM DTT, 0.2 mM phenylmethylsulfonyl fluoride (PMSF), 30 units/liter of Aprotinin, 0.2 M NaCl, and 10% glycerol. The homogenized cells were lysed in an ice cold French press and the lysate was centrifuged in a refrigerated centrifuge at 10,000 g for 40 min. All subsequent steps were carried out in a cold cabinet.

The supernatant was pumped onto a DEAE-cellulose column (DE23, 2 x 17.5 cm) at a flow rate of 0.75 ml/min to remove DNA. The column was washed with 135 ml of 20 mM Tris-HCl, pH 7.5; 1 mM EDTA; 1 mM DTT; 10% glycerol (buffer G) containing 0.2 M NaCl and then eluted with a 50 ml gradient to 1 M NaCl in buffer G; 15 min fractions were collected. Glycosylase activity appeared in fraction 5 and gradually tapered off to fraction 25. Fractions 5 through 13 were pooled and pumped at 0.7 ml/min onto a double stranded DNA cellulose column (1.5 x 9.5 cm) previously equilibrated with buffer G containing 0.2 M NaCl. The enzyme was eluted with an 80 ml gradient to 1 M NaCl in buffer G; 15 min fractions were collected. In addition to a broad peak near the front, a sharp peak of glycosylase activity was detected at fraction 18, approximately one third of the way through the gradient.

The peak fraction from the DNA-cellulose column was diluted to 72 ml with buffer G and pumped at 0.3 ml/min onto a P11 phosphocellulose column (2 x 8 cm) equilibrated with buffer G containing 0.15 M NaCl. The column was washed with 40 ml of buffer G containing 0.15 M NaCl and then eluted with an 80 ml gradient from 0.15 M to 1 M NaCl in buffer G. Again, 15 ml fractions were collected and immediately divided in half; 2 mg of serum albumin was added to one half to stabilize the glycosylase. Assays of these fractions showed a sharp peak of activity at fraction 27. SDS-PAGE analysis of this fraction showed that the enzyme had been concentrated in a band migrating at 39,000.

Studies of Glycosylase Action

Studies to measure glycosylase-mediated release of alkylated bases were performed in 70 mM Tris-HCl, pH 7.5, which contained 10 mM EDTA and 3 mM dithiothreitol. Incubations with [^{3}H]DMS-DNA contained 19.2 pmols of alkylated bases (14.0 pmols of 7-methyl guanine (m^7G) and 2.1 pmols of 3-methyl adenine (m^3A) in 22 μl of buffer. Experiments to determine enzyme dependence were incubated for 30 min; then, carrier DNA was added and substrate was precipitated by the addition of 1/20 volume of 6 M NaCl and 2 volumes of ethanol. An aliquot of the supernatant containing the released bases was evaporated to dryness and separated by HPLC to determine the amounts of MA and MG released. The time dependence of base release from [^{3}H]DMS-DNA was determined with 22 μl incubation mixtures containing 0.087 units of enzyme.

To compensate for its relatively low specific activity, incubations with [^{14}C]SM-DNA were performed at 6 times the scale of incubations with [^{3}H]DMS-DNA (i.e., with an incubation volume of 132 μl and with substrate containing 114 pmols of total alkylation). Incubation conditions were the same as described for [^{3}H]DMS-DNA, but the actual pmols of HETEG and HETEA that were released have been divided by 6 for direct comparison with the [^{3}H]DMS-DNA results. Because of the slightly different distribution of alkylated bases in [^{14}C]SM-DNA, there were 12.1 pmols of HETEG and 1.5 pmols of HETEA per 19.2 pmols of total alkylation in [^{14}C]SM-DNA.

Cell Culture Conditions

Human skin fibroblasts (AG01522B) obtained from the Coriell Institute for Medical Research, Camden, NJ were at a passage number of 6 and a population doubling level of 15. All experiments were performed with cells at a passage number between 8 and 10. Fibroblasts were grown as a monolayer in standard minimal essential media (MEM) with a 2 x concentration of amino acids and vitamins supplemented with 15% fetal bovine serum (FBS), penicillin and streptomycin. Cells were incubated in a humidified atmosphere of 7% CO_2 at 37°C.

Human keratinocytes (NM-1 cells) obtained from Dr. Howard P. Baden's laboratory, Massachusetts General Hospital, were at passage number 80. These cells were grown as monolayers in Serum Free Media (SFM) for keratinocytes from Gibco supplemented with bovine pituitary extract and epidermal growth factor. Chinese hamster ovary (CHO) cells were grown in Alfa minimum essential medium (Eagle) without ribonucleosides or deoxyribonucleosides, but supplemented with 10% FBS. Keratinocytes and CHO cells were grown in a humidified atmosphere of 7% CO_2 at 37°C. Incubation temperatures were monitored with a Yellow Springs Instrument Model 4600 digital thermometer.

Cytotoxicity Studies

Exposure Conditions

The cytotoxicity of SM was investigated by plating cells in 12-well plates at an initial density from 2 x 10^4 to 4 x 10^4 cells/cm^2. After 24 h for fibroblasts and CHO cells or 48 h for keratinocytes, the medium was replaced with fresh medium containing SM at the indicated concentration in a SterilchemGARD hood. Dilute solutions of SM in absolute alcohol were prepared immediately before treatment. Cell culture medium was replaced with fresh medium containing SM at the required concentration; cells were exposed to SM for 1 h at room temperature in the SterilchemGard hood and then incubated in fresh medium at 37°C. One half of the medium was changed every 2 days thereafter. At the indicated times, cell viability was determined. The effect of temperature on cytotoxicity was examined by incubating one set of plates for 1 or 2 days at a lower temperature before transferring them back to 37°C.

The effect of the cell cycle modulator, ciclopirox olamine (CPX), on cytotoxicity was examined by adding CPX dissolved in the medium to cells at the indicated times before and/or after exposure to the alkylating agent. After the required time, CPX was removed by replacing CPX-containing media with fresh medium.

Viability Assays

Trypan Blue Assay

For the trypan blue exclusion assay, cells were trypsinized, washed and resuspended in PBS. After staining, trypan blue-negative (excluding) cells were counted in a hemocytometer. Analysis of duplicate determinations shows that these counts are reproducible with a standard deviation of ± 6.3%.

Assay for Colony Forming Ability (CFA)

Based on the trypan blue excluding cell numbers obtained as described above, cells were diluted in growth medium and replated in five dilutions (from 50 to 2000 cells/well) in 6-well plates. After cells had been incubated for 10 to 14 days, the medium was discarded and colonies were rinsed with saline solution, fixed with ethanol, and stained with crystal violet. Colonies containing 50 or more cells were counted and colony forming ability was calculated as a percent of cells plated. For SM-exposed cells, CFA was expressed as a percent of control CFA. CFA of control cells remained at approximately 30% for several weeks.

Cell Cycle Analysis

The effect of sulfur mustard or potential modulators of cytotoxicity on cell cycle progression was examined by flow-cytometry. Cells grown in monolayers in 75 cm^2 flasks (~ 1 x 10^6 cells) were trypsinized after treatment, rinsed with PBS and resuspended in 0.1 ml of PBS. The cells were immediately fixed with 0.9 ml of ice-cold 95% ethanol and stored at 4°C for at least 24 h before analysis. Cells were stained by propidium iodide (PI) and fluorescence was measured using a FACScan flow cytometer (Becton & Dickinson, San Jose, CA).

RESULTS

Investigations into Alkylation of the O^6-Position of Guanine by SM

Synthesis of O^6-hydroxyethylthioethyl deoxyguanosine

Because of a significant body of literature emphasizing the cytotoxicity of O^6-guanine alkylation in DNA, we have been particularly interested in the possibility that SM might react with this position in DNA. Accordingly, the adduct that would be formed by such a reaction, O^6-hydroxyethylthioethyl deoxyguanosine, was synthesized by the reaction shown below.

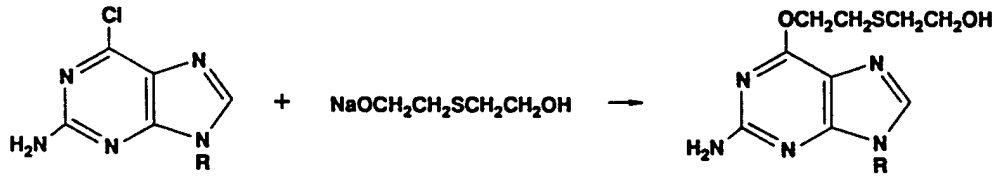

Figure 3. Synthesis of O^6-Hydroxyethylthioethyl Deoxyguanosine.

The structure of this compound was established by its uv spectra which are typical of an O^6-substituted guanine nucleoside, and by its FABMS molecular weight of 371 confirming the nature of the substituent.

With this marker available, it was possible to demonstrate that O^6-hydroxyethylthioethyl deoxyguanosine was formed when SM reacted with deoxyguanosine. Deoxyguanosine (2 mg) was reacted with HSM (4 μl) for 4 h at 37°C in 50 mM

sodium cacodylate buffer, pH 7. The mixture was then analyzed on a C_{18} column eluted with an acetonitrile gradient. As shown in Figure 4, a small peak eluted at 82 min which was identified as O^6-hydroxyethylthioethyl deoxyguanosine on the basis of its retention time, its uv spectrum as captured on a diode array detector, and its intense fluorescence.

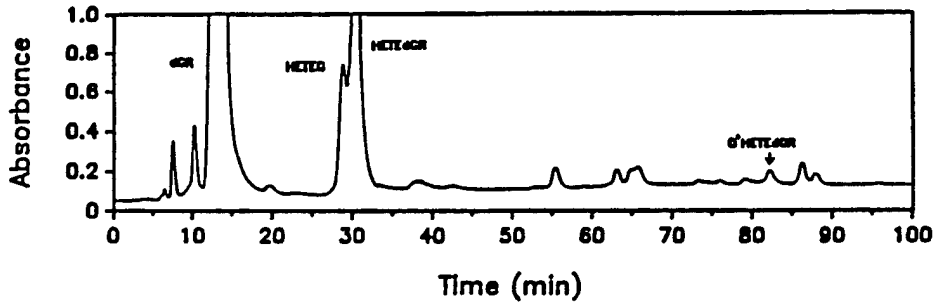

Figure 4. HPLC Profile of Sulfur Mustard-Deoxyguanosine Reaction Mixture. A small peak of O^6-hydroxyethylthioethyl deoxyguanosine appeared at 82 min.

In order to demonstrate the presence of O^6-hydroxyethylthioethyl deoxyguanosine in DNA that has been reacted with HSM or SM, it is necessary to release the adduct from DNA as a monomer either by acid hydrolysis or enzymatic digestion. Acid hydrolysis would release the free base, O^6-hydroxyethylthioethyl guanine (O^6-HETEG) while enzymatic digestion would release O^6-hydroxyethyl thioethyl deoxyguanosine monophosphate. When we failed to obtain evidence for the presence of this adduct in SM-treated DNA, we performed the control experiments shown in Figure 5 (next page) to see whether the adduct was stable under hydrolysis or digestion conditions. As shown in the top panel of Figure 5, synthetic O^6-HETEG appeared as a late peak in the HPLC profile. When O^6-HETEG was subjected to standard acid hydrolysis conditions (90°C for 1 h at pH 3.5), it was converted entirely to guanine as shown in the middle panel of this figure. Similar results were obtained using alternate acid hydrolysis conditions (37°C for 18 h at pH 1). Finally, as shown in the bottom panel of Figure 5, O^6-HETEG was unstable under enzyme digestion conditions (37°C for 18 h at pH 7.5). As would be expected, the deoxynucleoside, O^6-hydroxyethylthioethyl deoxyguanosine, was also unstable under enzyme digestion conditions.

Thus, we conclude that it would not be possible to determine whether an O^6-guanine adduct is formed in DNA by SM through the use of either standard hydrolysis or enzyme digestion conditions. We have found, however, that O^6-hydroxyethylthioethyl deoxyguanosine remains approximately 50 % intact after exposure to the 10°C digestion conditions that we use in the ^{32}P-postlabeling procedure. Accordingly, it might be possible to obtain a more definite answer as to whether O^6-guanine adducts are formed by performing the digestion in this way. This demonstration will require synthesis of the HPLC marker that would be expected from enzymatic digestion, O^6-hydroxyethylthioethyl deoxyguanosine 5'-phosphate.

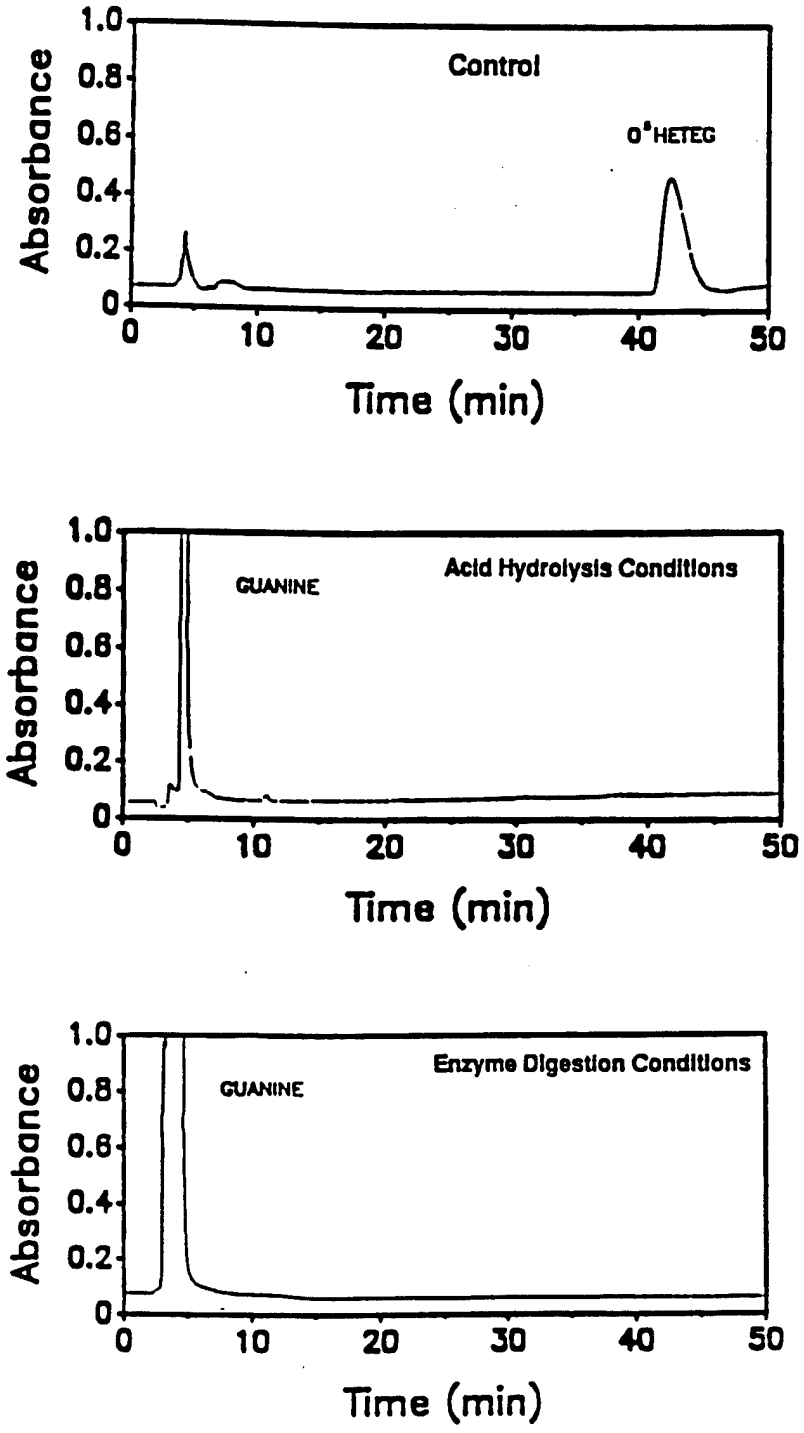

Figure 5. Instability of O^6-HETEG Under Standard Acid Hydrolysis and Enzyme Digestion Conditions. Synthetic O^6-HETEG appeared at approximately 42 min when it was eluted from an C_{18} column with an acetonitrile gradient as shown in the top panel. When marker O^6-HETEG was subjected to acid hydrolysis conditions (middle panel) or enzymatic digestion conditions (bottom panel) it was converted entirely to guanine.

^{32}P-Postlabeling Analysis of SM-induced DNA Modifications

Our ^{32}P-postlabeling technique has been improved substantially since our last final report (37) and can now detect HETEpdG at the level of one modification in 10^7 DNA nucleotides. These improvements have been achieved by including an internal standard with HPLC and stability characteristics similar to those of HETEdGp from the beginning of the analysis, and by making more extensive use of disposable A-25 cartridges to separate HETEdGp from unmodified deoxynucleotide 3'-phosphates (step 2 in Figure 1) as well as from [^{32}P]ATP (step 5).

As shown in Table 1, the disposable A-25 columns separate nucleotides into three groups: 7-substituted guanine nucleotides that elute between 14 and 16 min, unsubstituted nucleotides that elute between 35 and 71 min, and ATP that is retained on the column. Consequently, similar columns can be used in both the HETEdGp enrichment step 2 and the ATP removal step 5. BupdG was added as an optical marker in step 2 and HETEpdG as an optical marker in steps 5 and 6. The nature of the alkyl substituent, n-butyl, was chosen to produce a satisfactory separation during the final HPLC analysis, step 6.

Table 1. Retention Times on Disposable Sephadex A-25 Columns

Nucleotide	Retention time (min)	Nucleotide	Retention time (min)
HETEdGp	15.7	dTp	35
HETEpdG	15.3	dCp	41
BudGp	14.3	dAp	50
BupdG	14.6	dGp	71
		ATP	> 120

Figure 6 (next page) is an example of the assay. An aliquot of a digest from 1 nmol of [^{14}C]SM-DNA that contained 2 fmol of BudGp as internal standard was separated on a C_{18} column. From our computer program, HETEpdG radioactivity equaled 0.75 times BupdG radioactivity, indicating that 1.5 fmol of HETEpdG were present. Separately, however, we had determined from its [^{14}C] content that 1 nmol of this [^{14}C]SM-DNA blend originally contained 10.2 fmol of HETEpdG. Consequently, the overall recovery of HETEpdG in the analysis was 15%. However, by increasing the amount of DNA analyzed to 40 nmol (13.2 μg), it was possible to measure the HETEpdG content of [^{14}C]SM-DNA blends containing as little as one HETEpdG/10^7 DNA nucleotide accurately.

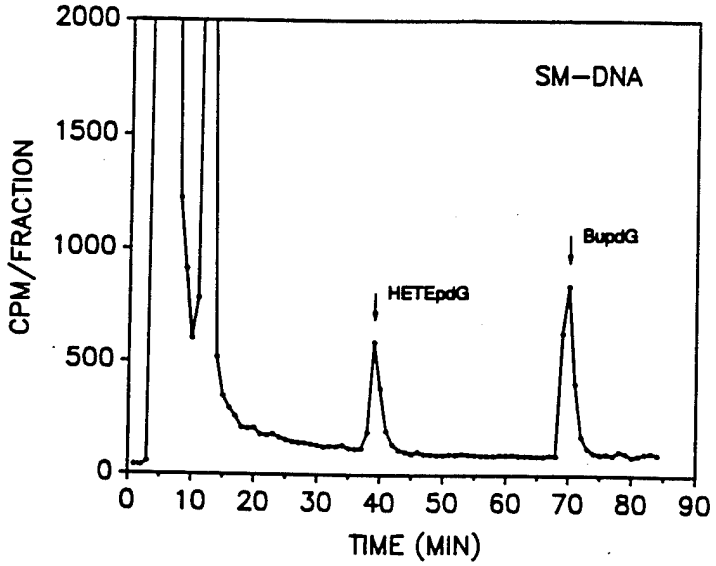

Figure 6. HPLC Profiles Showing Detection of 1.5 fmol of HETEpdG. Top panel, labeled digest from 1 nmol (0.3 μg) of [^{14}C]SM-DNA to which 2 fmol of BudGp was added as internal standard. Bottom panel, labeled digest from 1 nmol (0.3 μg) of unmodified DNA with 2 fmol of BudGp added.

To test the reproducibility of the assay, a representative blend containing 5.2 fmol HETEpdG per nmol of DNA was analyzed a total of four times by two different operators. Recoveries were 13.0%, 20.7%, 21.7%, and 25.6% for a mean of 20.2 ± 5.2.

The calibration curve obtained by analyzing a range of blends containing from 8.7×10^{-8} to 3.1×10^{-5} HETEG per DNA nucleotide is shown in Figure 7 (next page). The data show a linear dependence of the log of HETEpdG recovered on the log of HETEpdG in the DNA blend analyzed. The actual relationship is given by the equation: $\log y = 2.47 + 1.61 \log x$ with a correlation coefficient of 0.99.

Although the ^{32}P-postlabeling method described above is satisfactory for the detection of HETEpdG *in vitro*, irreproducible results were obtained initially when the method was applied to DNA that had been isolated from human fibroblasts. This irreproducibility was traced to the effects of extraction with organic solvents, a step that is included in most standard DNA isolation procedures (48). By analyzing DNA samples that had been modified by SM *in vitro*, we were able to demonstrate that extraction with organic solvents drastically reduced the apparent HETEpdG content (data not shown). Apparently the lipid solubility of the hydroxyethylthioethyl group is sufficient to allow hydroxyethylthioethyl-substituted nucleotides or oligonucleotides to be extracted from the remainder of the DNA. When we substituted a salt precipitation step for protein removal (45), reproducible results were obtained.

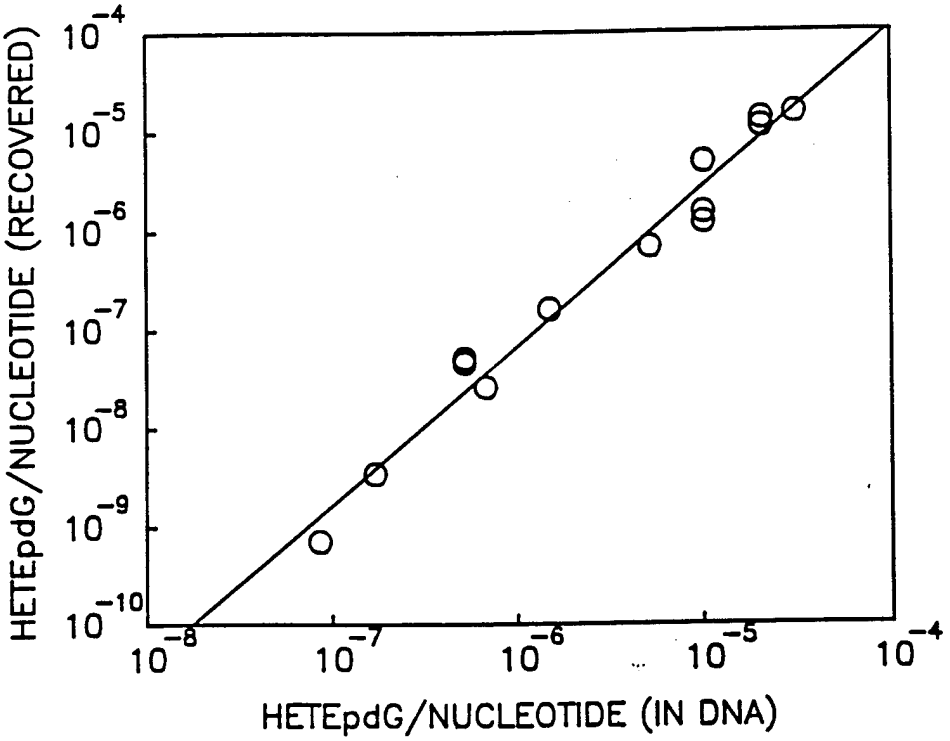

Figure 7. Calibration Curve for Detecting HETEpdG in DNA. Samples of DNA containing the indicated ratio of HETEpdG to normal nucleotides were digested and labeled in the presence of internal standard; the calculated amount of HETEpdG recovered is plotted on the y axis.

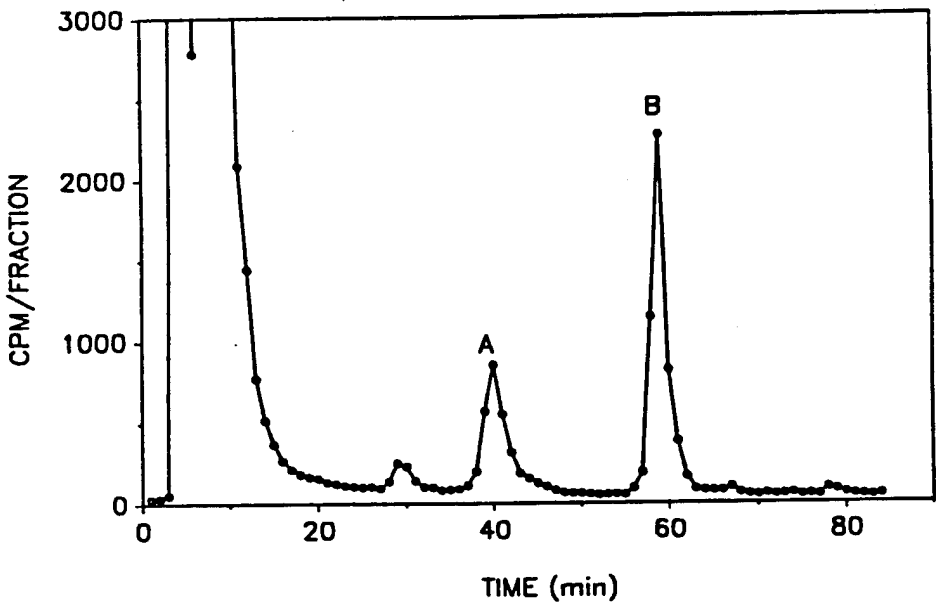

Figure 8. HPLC Profile of ^{32}P-postlabeled Nucleotides from the DNA of Fibroblasts Exposed to 10 μM SM. DNA was isolated, digested in the presence of BudGp, and the resulting nucleotides were labeled and separated on a C_{18} column eluted as described in Methods. Positions of optical markers for HETEpdG (A) and BupdG (B) are indicated.

A typical HPLC profile showing the analysis of HETEpdG in DNA extracted from fibroblasts exposed to 10 μM SM is shown in Figure 8. The peaks of radioactivity corresponding to HETEpdG and BupdG are clearly evident and are well resolved from each other. The peak in the front is inorganic ^{32}P-phosphate and ^{32}P-deoxyribose 5'-phosphate while the small peak at 30 min is not present in the reagent blank and probably represents another SM-induced adduct. The sensitivity of the assay is more than adequate for measurements at this level of modification and could be increased if necessary by increasing the amount of DNA analyzed.

Table 2 shows the results of HETEpdG analyses on DNA samples isolated from fibroblasts exposed to concentrations of SM from 0 to 15 μM. The third column in this table gives the number of independent postlabeling assays, n, which were performed on a single DNA isolated at each SM concentration except for the control at 0 μM SM. For that sample, two separately isolated samples were analyzed. The data in the fourth column are the actual values of HETEpdG recovered in the analysis while those in the fifth column are the original values calculated from the mean values in column 4 using the calibration curve shown in Figure 7.

Table 2. Calculated HETEpdG Levels in DNA of Fibroblasts Exposed to SM

Sample	SM (μM)	n	Recovered HETEpdG per 10^6 nucleotides[a]	Calculated HETEpdG per 10^6 nucleotides
Reagent blank	0	4	0.052 ± 0.028	-
Fibroblast DNA	0	3	0.039 ± 0.030	0
Fibroblast DNA	2.5	2	0.166, 0.200	1.61
Fibroblast DNA	5.0	2	0.120, 0.178	1.37
Fibroblast DNA	10.0	3	0.569 ± 0.241	3.63
Fibroblast DNA	15.0	3	0.577 ± 0.168	4.08

[a]Mean ± SD. Individual values are given when n = 2.

A small reagent blank was subtracted from the values in the fourth column of Table 2 before applying the calibration curve. This blank apparently arose from a slight contaminant in the ^{32}P-ATP which was not removed by the anion exchange column. An alternate possibility is that the internal standard, BudGp, was slightly contaminated with a nucleotide that coeluted with HETEpdG after it was labeled.

The data in table 2 indicate that the HETEpdG levels in DNA isolated from fibroblasts have a linear dependence on the SM concentration. This relation-

ship is given by the equation: HETEpdG = 0.396 + 0.268 SM with a correlation coefficient of 0.95. HETEpdG in this equation is the number of adducts per 10^6 nucleotides and SM is the μM concentration of SM. This relationship indicates that one HETEpdG per 10^6 nucleotides is produced at a SM concentration of 2.3 μM, a level that causes a slight inhibition of growth as described in a later section of this report.

Repair of SM-induced DNA Modifications

We have obtained evidence for repair of SM-induced DNA modifications from *in vitro* as well as *in vivo* experiments. In this section, we report biochemical studies showing that both bacterial and human glycosylase recognize and release HETEG and HETEA from SM-modified DNA. In a later section we report cytotoxicity studies indicating that nucleotide excision repair (NER) plays a role in protecting mammalian cells from the cytotoxic action of SM. O^6-Alkylguanine-DNA alkyltransferase activity does not, however, seem to be effective in preventing cytotoxicity.

[^{14}C]SM-DNA and [^{3}H]DMS-DNA for use in glycosylase studies were prepared by reacting the radiolabeled alkylating agents with DNA as described in Methods. To determine the content and distribution of alkylated bases in these substrates, [^{14}C]SM-DNA was depurinated by adjusting the pH to 3.5 with H_3PO_4 and incubating at 90° for 1 h. [^{3}H]DMS-DNA was depurinated by overnight incubation in 0.1 N HCl at 37°C. Optical markers were added and modified bases were separated by HPLC; 1 min fractions were collected and counted in an LKB model 1214 liquid scintillation counter. Compositions of these two substrates are given in Table 3 below.

Table 3. Characteristics of Alkylated Substrates

Property	[^{3}H]DMS-DNA	[^{14}C]SM-DNA
dpm/μg	6946	4726
pmol/μg	1.75	33.3
7-alkylguanine (pmol/μg)	1.28	21.1
3-alkyladenine (pmol/μg)	0.193	2.6
ratio, 7-RG/3-RA	6.6	8.1
cross-link (pmol/μg)	-	6.5

These substrates had a similar number of dpm/μg of DNA, but because of the much higher specific activity of the methyl groups, there were fewer pmols of methylated bases per μg of DNA in the [^{3}H]DMS-DNA than in [^{14}C]SM-DNA. However, the ratio of 7-alkylguanine to 3-alkyladenine bases in the two substrates was rather similar. The distribution of adducts in the acid hydrolysate of [^{14}C]SM-DNA shown in the left-hand panel of Figure 9 (next page) and in Table 3 is similar to that which has been reported previously (13,16). The substrate used here contained, as a percentage of total alkylation, 7.7% HETEA, 63% HETEG, and 19.5% cross-link (di-(2-guanin-7-yl-ethyl)sulfide).

Figure 9 shows HPLC profiles of bases released from [^{14}C]SM-DNA by acid, and by the action of 3-methyladenine DNA glycosylase II (Gly II). As shown in the right-hand panel of this figure, a 15 min incubation at 37° with Gly II released both HETEA and HETEG, but there was no evidence for release of the cross-link. There was very little spontaneous release (middle panel) of either modified base under these incubation conditions.

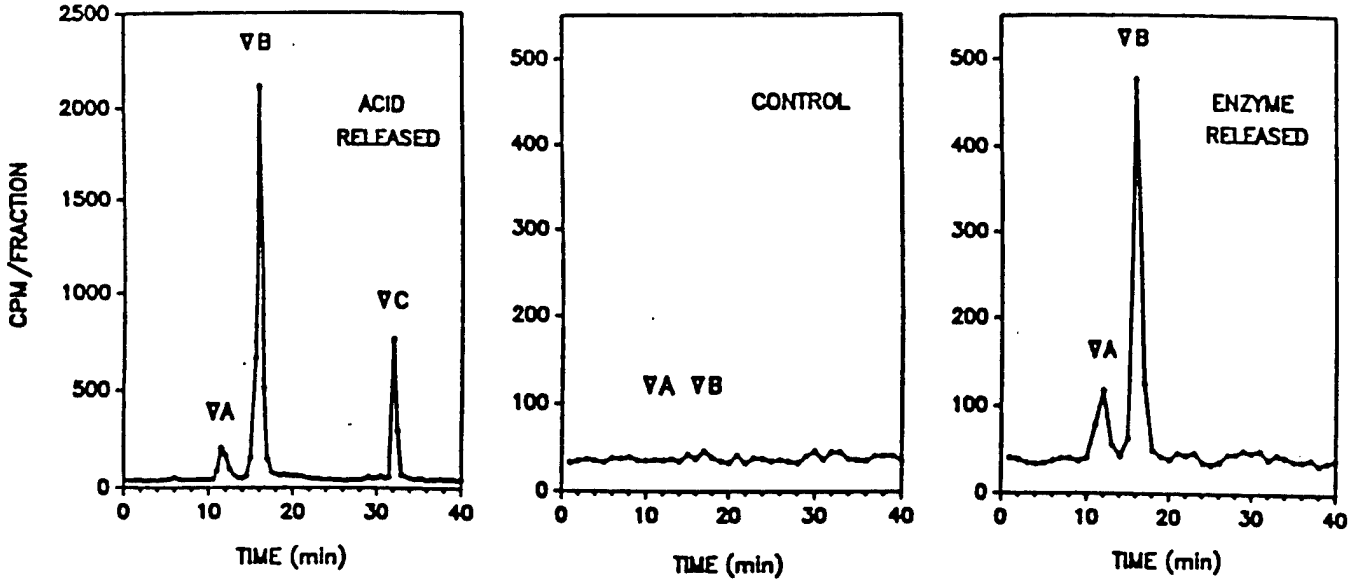

Figure 9. HPLC Profiles of Bases Released from SM-modified DNA (see text). Retention times are indicated for optical markers of: A, HETEA; B, HETEG; and C, cross-link. The panels from left to right show radioactivity released by acid depurination, control incubation with buffer alone, or incubation with 3-methyladenine DNA glycosylase II.

To establish the enzyme dependence of this release, and to compare the activity of Gly II towards SM-modified bases with its activity towards methylated bases, experiments were performed as shown in Figures 10 and 11. Gly II releases both m^3A and m^7G readily from the methylated substrate as shown in the left-hand panel of Figure 10. Although the amount of m^7G released is approximately one third of the amount of m^3A released, the much greater activity of this enzyme towards m^3A than m^7G becomes apparent when these data are expressed as percentages. As shown in the right-hand panel of Figure 10, approximately 80% of the m^3A is released at the highest enzyme concentration while only approximately 5% of the m^7G is released.

However, Gly II has a relatively much greater activity towards HETEG than m^7G as shown in Figure 11. The left-hand panel of this figure shows that more HETEG than HETEA is released at each enzyme concentration - the reverse of what happens with a methylated substrate where more m^3A than m^7G is released. A comparison of the left-hand panel of Figure 10 with the left-hand panel of Figure 11 indicates that approximately twice as much m^3A as HETEA is released at each enzyme concentration, but more than three times as much HETEG as m^7G is released.

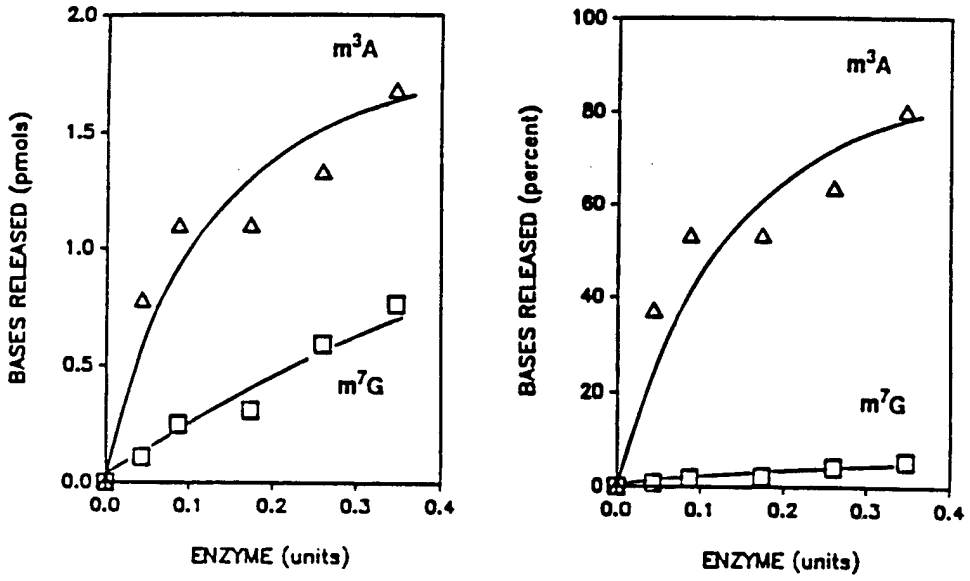

Figure 10. Enzyme-dependent Release of Methylated Bases by 3-methyladenine DNA Glycosylase II. Substrate was incubated with enzyme for 30 min at 37°C (see text for details). The left-hand panel shows the pmols of each base released from a substrate containing a total of 19.2 pmols of modified bases, and the right-hand panel shows the percent of each base released.

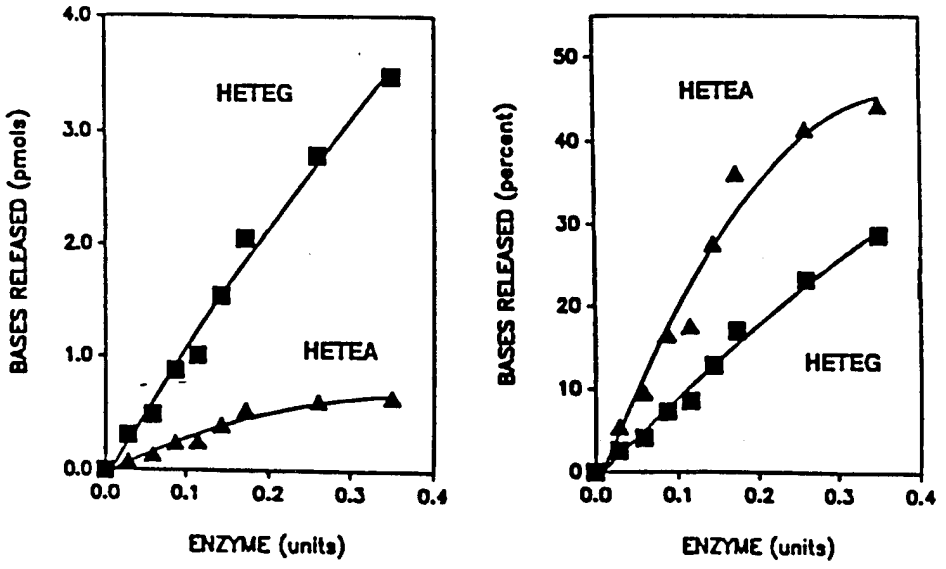

Figure 11. Enzyme-dependent Release of SM-modified Bases by 3-methyladenine DNA Glycosylase II. Substrate was incubated with enzyme for 30 min at 37°C (see text for details). Left and right panels as in Figure 10.

When the data in Figure 11 are expressed as a percentage of bases released (right hand panel of figure), it is apparent that a higher percent of HETEA is released than HETEG, but the preference of the enzyme for HETEA over HETEG is not as great as the preference for m^3A over m^7G. On a percentage basis, only about one sixteenth as much m^7G is released as m^3A, but more than half as much HETEG is released as HETEA.

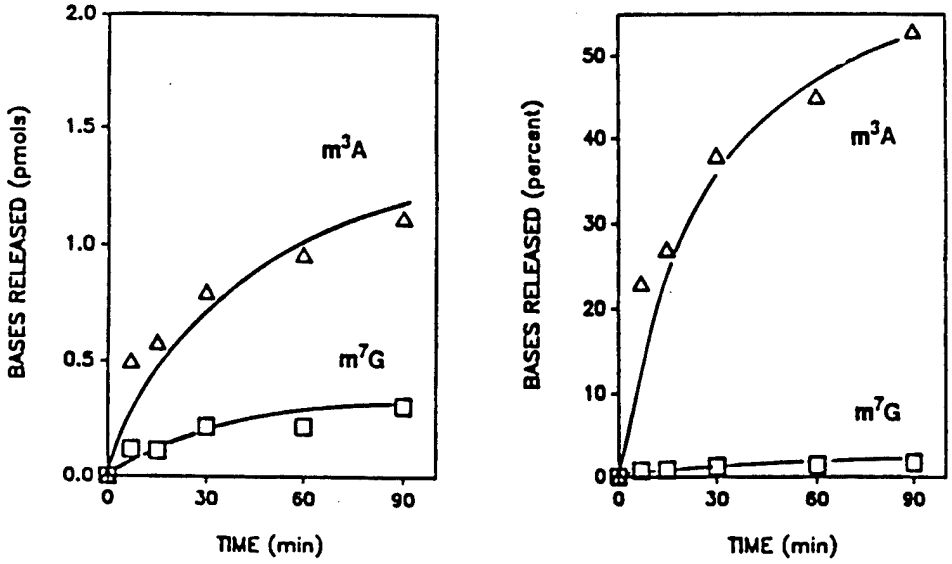

Figure 12. Time-dependent Release of Methylated Bases by 3-methyladenine DNA Glycosylase II. Substrate was incubated with enzyme for varying times at 37°C (see text for details). Left and right panels as in Figure 10.

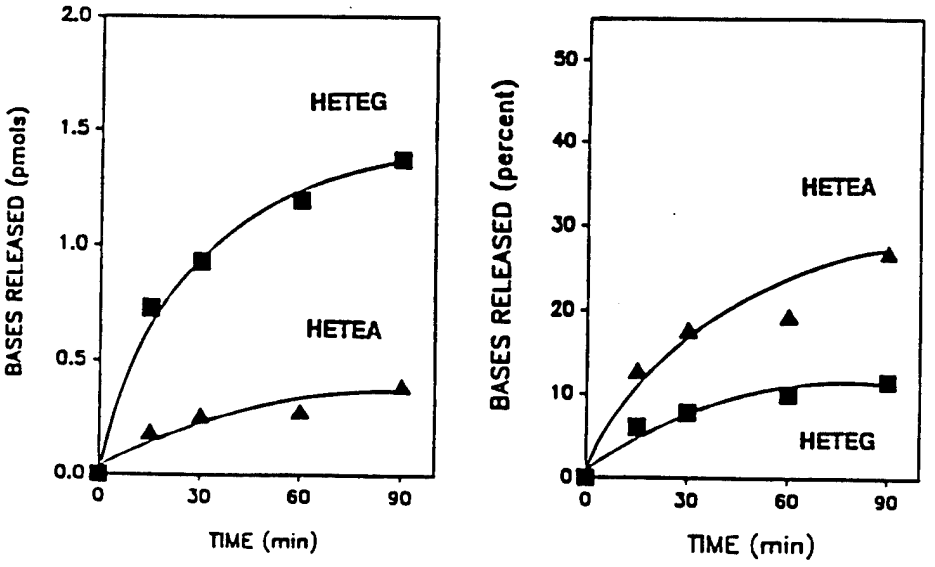

Figure 13. Time-dependent Release of SM-modified Bases by 3-methyladenine DNA Glycosylase II. Substrate was incubated with enzyme for varying times at 37°C (see text for details). Left and right panels as in Figure 10.

Time dependence experiments shown in Figures 12 and 13 lead to similar conclusions. Data for the methylated substrate are shown in Figure 12; the rapid release of m^3A in comparison with m^7G is apparent. Again, the difference is magnified when the data are expressed as percentages of bases present in the substrate.

For the hydroxyethylthioethyl bases, however, more HETEG is released than HETEA throughout the time course. Again, because there is approximately eight times as much HETEG as HETEA in the substrate (see Table 3), HETEG is released somewhat more slowly than HETEA on a percentage basis. However, in comparing the right-hand panel of Figure 13 with the right-hand panel of Figure 12, the much greater activity of this enzyme towards HETEG than m^7G is again clearly illustrated.

The results reported above with bacterial enzyme raise the possibility that glycosylase may play an important role in the repair of SM-induced DNA modifications in human cells. Accordingly, we have begun studies of the action of human glycosylase on the same [^{14}C]SM-DNA substrate that we used for the bacterial glycosylase experiments.

Figure 14 shows preliminary results with partially purified enzyme. Incubation of the substrate with buffer alone (left hand panel of Figure 14) results in some spontaneous release of both HETEA and HETEG. However, the addition of either 75 or 150 μl of partially purified human enzyme increases the release of both peaks in a dose-dependent manner. Thus we conclude that human glycosylase may play an important role in protecting cells from SM toxicity.

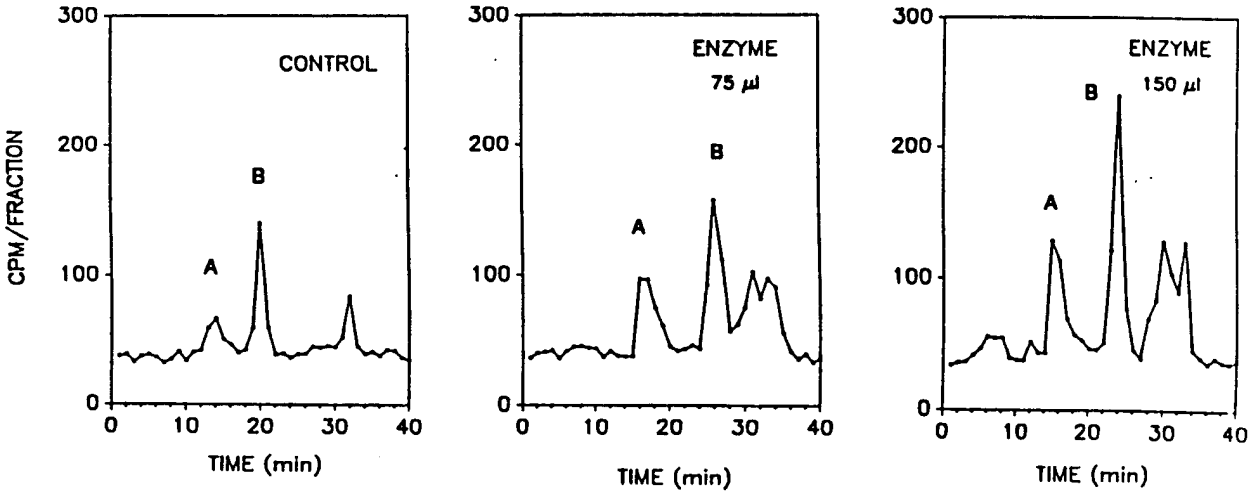

Figure 14. HPLC Profiles of Bases Released from ^{14}C-SM-DNA. Approximately 16,300 cpm's of ^{14}C-SM-DNA were incubated with 0, 75 or 150 μl of cloned, partially purified human glycosylase for 60 min at 37°C. Peak identities: Peak A, HETEA; Peak B, HETEG.

Cytotoxicity Studies

Effects of SM on Cell Growth

SM is acutely toxic to human fibroblasts as shown in Figure 15. In the absence of SM exposure, cells grow to confluency in less than one week while exposure to even 1 μM SM slows growth considerably, particularly in the first few days. At SM concentrations as high as 20 μM, cell growth is inhibited for a very long time but eventually recovers.

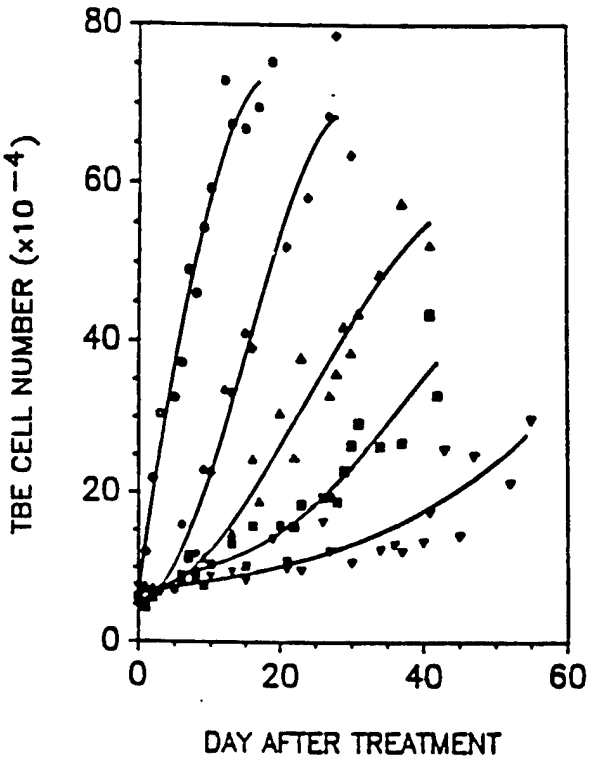

Figure 15. Effect of SM on Growth of Human Fibroblasts. Twenty four h after plating (day 0) cells were exposed to 0 μM (●), 1 μM (♦), 5 μM (▲), 10 μM (■), or 20 μM (▼) SM at room temperature. After 1 h exposure, the medium was changed and the cells were incubated at 37°C; viability was determined by the TBE assay as shown. Points are the mean values from 2 to 4 independent experiments.

The SM-induced delay in cell growth shown in Figure 15 depends on the SM concentration to which the cells were exposed. This is evident from Figure 16 (next page) in which the time required for the first doubling of cell population (determined from graphs of the TBE number *versus* time) is plotted against sulfur mustard concentration. The time required for the first doubling of the TBE number shows an almost linear dependence on SM concentration.

The appearance of fibroblasts exposed to SM changes markedly with time as shown in Figure 17 (next page). This figure shows progressive changes in appearance of cells exposed to 10 μM SM over several weeks in comparison with unexposed cells. After exposure, cells increase greatly in size and show evidence of "unbalanced growth". Later, when they begin to divide again, they return to a more normal appearance.

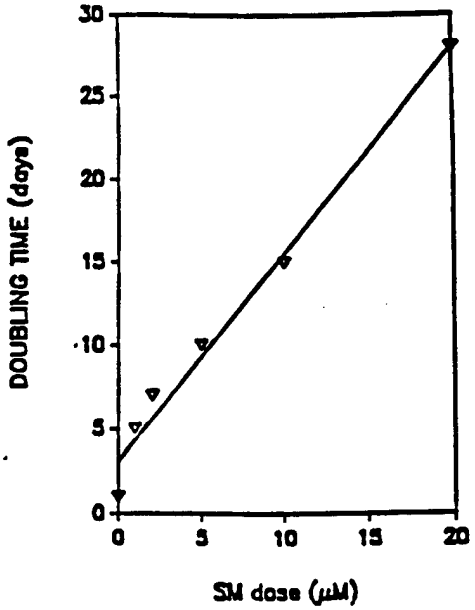

Figure 16. Dependence of Growth Inhibition on SM Concentration. The time required for the first population doubling after exposure, determined from growth curves as shown in Figure 15, is plotted against SM concentration.

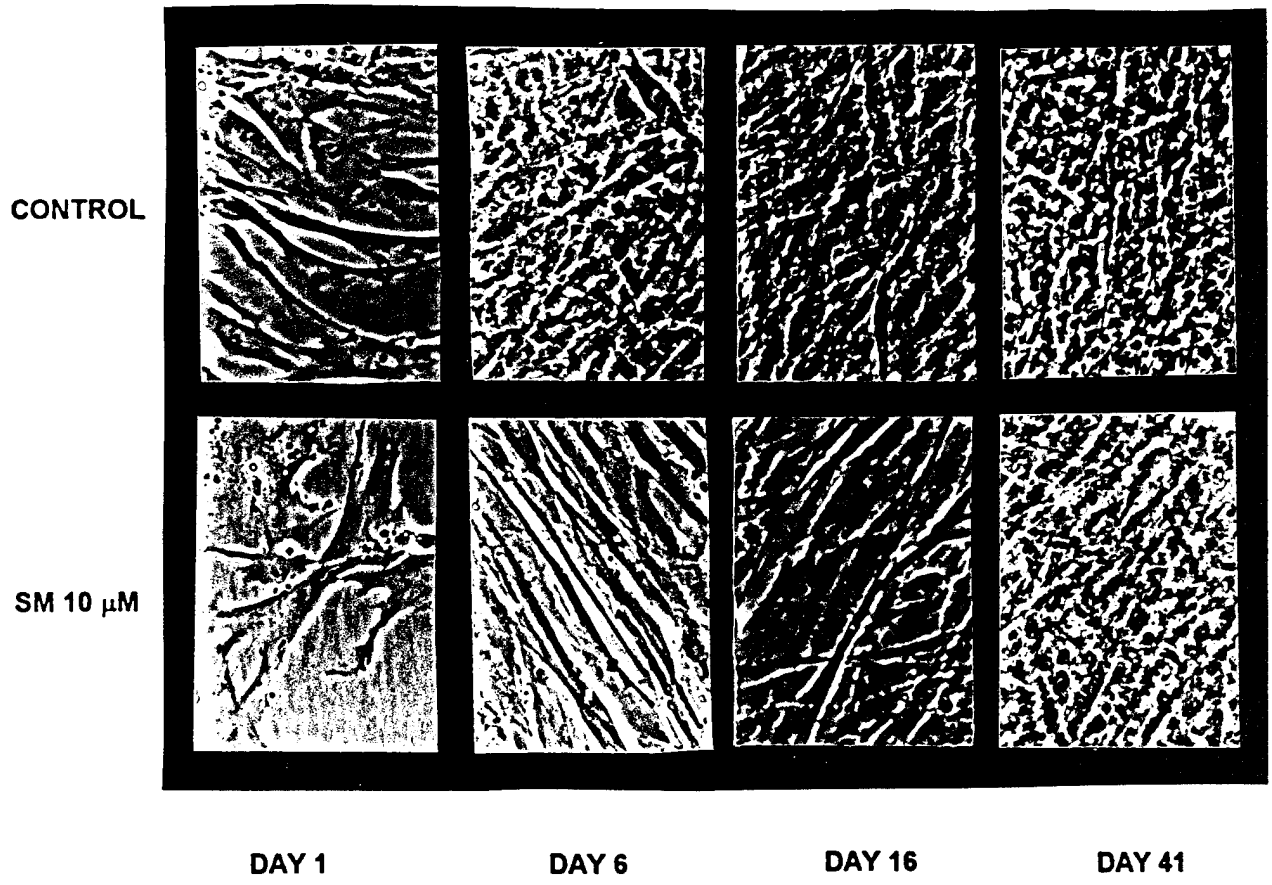

Figure 17. Effect of SM on Fibroblast Appearance. Cells grown in a monolayer at a density of 1 x $10^4/cm^2$ were exposed to 10 μM SM at room temperature. After 1 h exposure, the medium was changed and the cells were incubated at 37°C. Top row, control cells; bottom row, SM-treated cells. Magnification: 400 x.

The effect of SM on cell size is shown in Figure 18 where the relative size of fibroblasts is plotted *versus* time after exposure. For cells exposed to 5 μM SM, the relative size almost triples, reaching a maximum approximately two weeks after exposure. After that, cells begin to divide again and return to their original size and appearance.

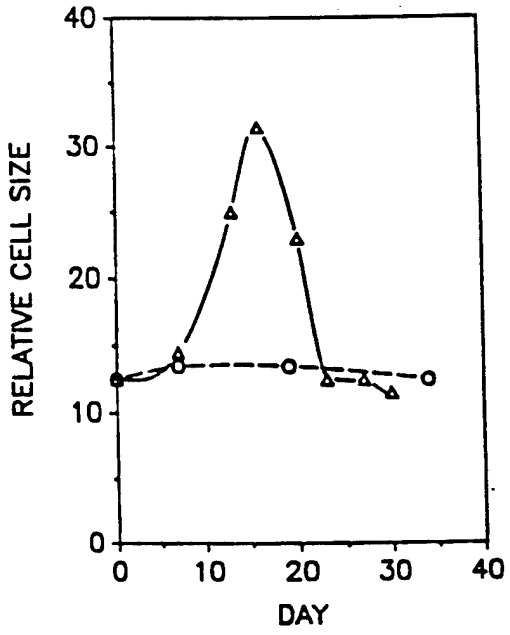

Figure 18. Relative Change in Size after Exposure to SM. Cells were exposed to 5 μM SM at room temperature for 1 h. The medium was changed and the cells were incubated at 37°C until they were harvested by trypsinization at the indicated times. Cell size was estimated from the spacing of the grids in the hemocytometer. Symbols: (Δ), cells exposed to SM; (O), Control, unexposed cells.

Although the slow increase in number of TBE cells which is observed after SM exposure could represent a balance between cell division and cell death, no significant cell detachment or dose-dependent increase in the number of trypan blue non-excluding cells was observed during the recovery period even at the highest concentrations of SM tested. We conclude, therefore, that the period of growth arrest represents a period in which most cells are not dividing and does not represent a dynamic balance between dividing and dying cells.

Colony forming ability (CFA) as well as TBE number was followed after exposure to varying concentrations of SM. Figure 19 (next page) shows CFA *versus* SM concentration at day 1, day 9, and day 31 after exposure. CFA in this graph is plotted as a percentage of CFA for unexposed cells. Each of these curves shows a dose-dependent decrease in CFA, but at any SM concentration, CFA returns to more normal levels by day 9 and especially by day 31. In these CFA experiments, there was no apparent difference in size among the colonies formed at any time after exposure. Furthermore, cells within the colonies that were derived from SM-treated and those from control populations had a similar appearance. Thus, the CFA experiments also suggest that cells may return to a normal condition after a temporary growth arrest.

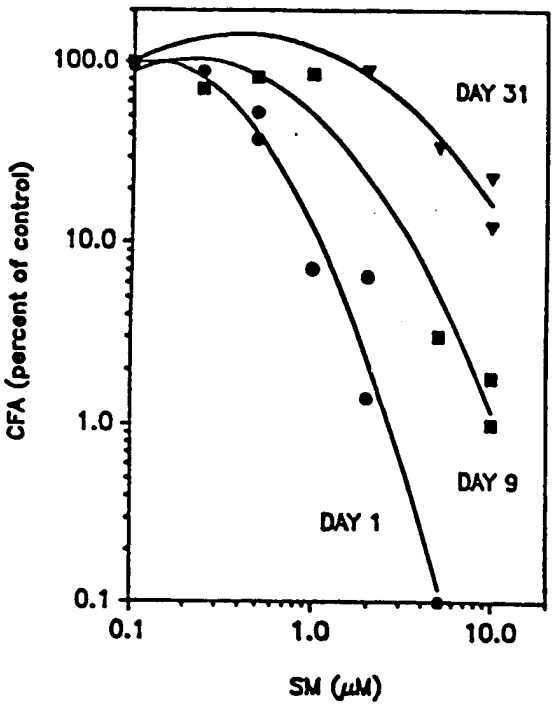

Figure 19. Recovery of Colony Forming Ability (CFA) after Exposure to SM. Human fibroblasts were exposed to the indicated concentrations of SM at room temperature. After 1 h exposure, the medium was changed and the cells were incubated at 37°C. After 1, 9, or 31 d, they were harvested and replated in serial dilutions for CFA. After incubation at 37°C for 12 days, colonies were stained with crystal violet and counted; CFA is expressed as a percent of CFA for untreated controls.

Different cells respond to SM in different ways, however. We have studied Chinese hamster ovary (CHO) cells because several repair-deficient lines are available for investigations of DNA repair. As shown in the left-hand panel of Figure 20 (next page), the growth of these cells as measured by TBE number is also affected by low levels of SM. In contrast to fibroblasts, however, there is clear evidence for cell death with the appearance of cells that do not exclude trypan blue. As shown in the right-hand panel of Figure 20, more than half of the CHO cells exposed to 5 μM SM are considered dead by the TBE assay within a few days of exposure. As discussed below, we believe that the ability of cells to recover may depend on their ability to arrest growth at various checkpoints until DNA repair is complete.

We have also investigated the toxicity of SM towards a line of human keratinocytes that we have obtained from Dr. Howard Baden. This cell line grows more slowly than either the fibroblasts or the CHO cells as shown in Figure 21 (next page). They also appear even more sensitive to SM than either the fibroblasts or CHO cells. As shown in Figure 21, 5 μM SM arrests these cells for at least two weeks after exposure. In order to investigate the interrelationship between DNA repair and cell growth, however, we have emphasized studies of fibroblasts and CHO cells.

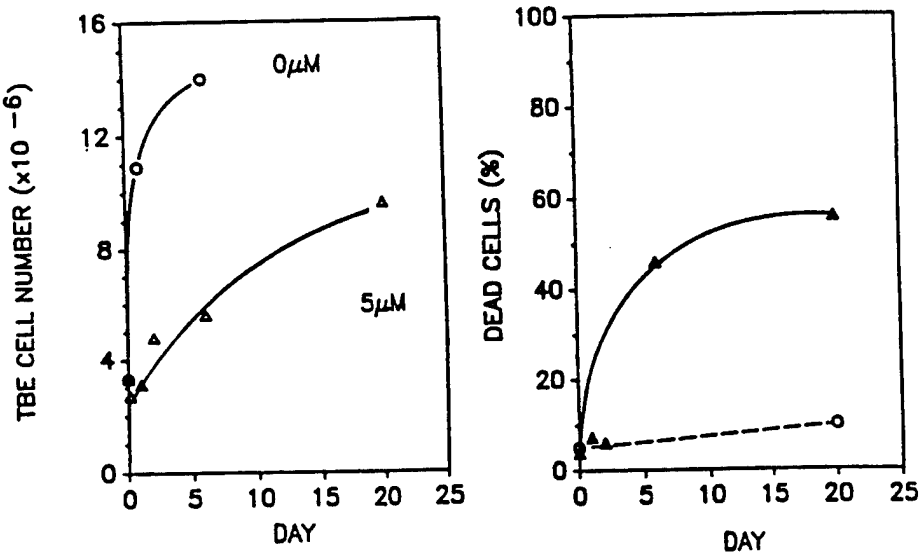

Figure 20. Effect of SM on Growth of CHO Cells. After CHO cells were exposed to 5 μM SM for 1 h, the medium was changed and the cells were incubated at 37°C. Left-hand panel, number of trypan blue excluding (viable) cells; right-hand panel, percent of trypan blue non-excluding (dead) cells. For comparison, the percent of trypan blue non-excluding fibroblasts after exposure to the same dose is shown as a dashed line in the right-hand panel.

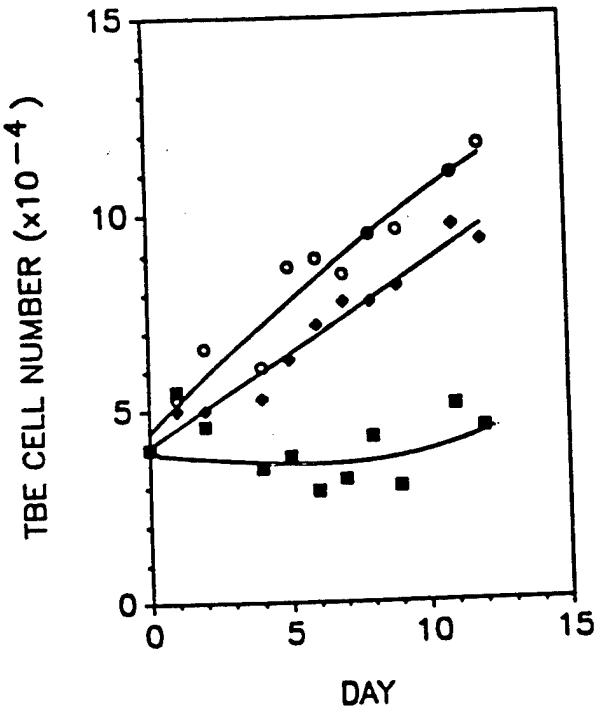

Figure 21. Effect of SM on Growth of Human Keratinocytes. Two days after plating, cells grown in a monolayer were exposed to 0 μM (○), 1 μM (♦) or 5 μM (■) SM at room temperature. After 1 h exposure, the medium was changed and the cells were incubated at 37°C; viability was determined by the TBE assay.

Effects of SM on Cell Cycle Distribution

SM exposure produces dose-dependent changes in the cell cycle distribution as shown in Figure 22. This figure compares cell cycle distributions of asynchronous fibroblasts one day after exposure to varying concentrations of SM with the cell cycle distribution of control cells. On day zero (time of exposure), control cells shown at the top of this figure are beginning to enter the S phase. On day one, the distribution is typical of rapidly dividing cells with a significant G_2 as well as G_1 peak.

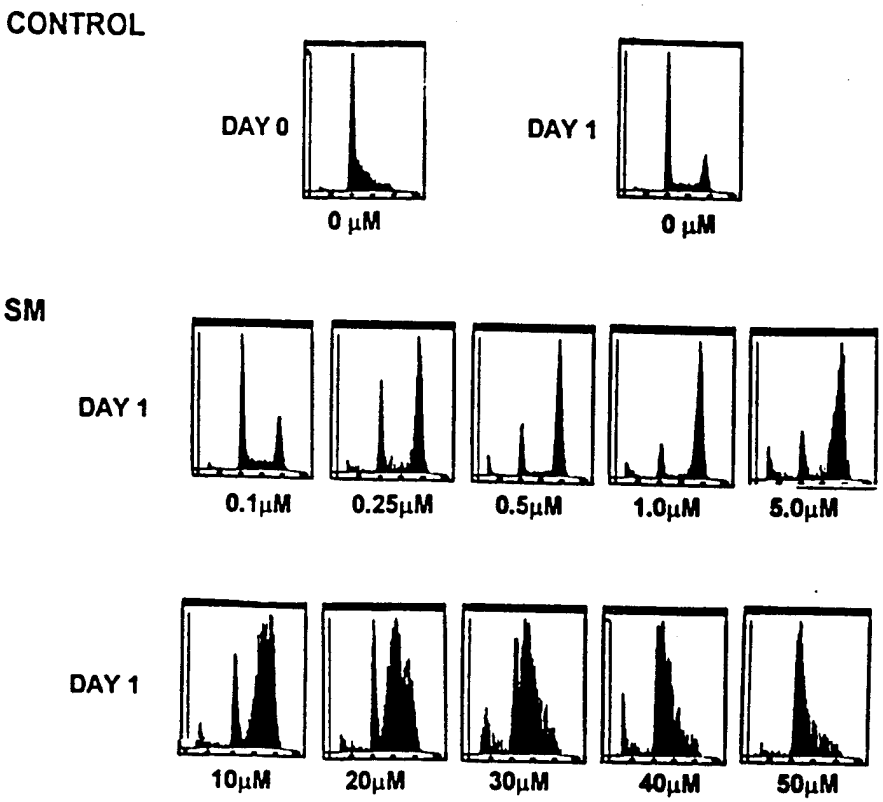

Figure 22. Effect of SM on Cell Cycle Distribution. Asynchronized fibroblasts grown in a monolayer were exposed to varying concentrations of SM for 1 h at room temperature. After the medium was changed, the cells were incubated at 37°C; 24 h later, cell cycle analysis was performed as described in Methods. Top row: Cell cycle distribution in control cells on the day of treatment (day 0) and 24 h later (day 1). Bottom two rows: Cell cycle distribution on day 1 for cells exposed to the indicated concentration of SM.

SM-exposed cells show an altered distribution on day one which is strongly dose-dependent. At the lowest concentrations of SM, there is a G_2 arrest. At concentrations above 10 μM, however, an increasingly large fraction of the cells are arrested in G_1. We are particularly interested in the G_2 arrest seen at lower concentrations, because we believe that this may represent a compensatory response which would allow cells to repair their DNA damage and recover from low levels of exposure.

The percentage of cells in each phase of the cell cycle distributions shown in Figure 22 is given as a function of SM exposure concentrations in Figure 23. Cells exposed to the lowest dose of SM have approximately 50% of their cells in G_1, 20% in S, and 30% in G_2. As the SM dose is increased to approximately 1 μM, the number of cells in G_1 decreases while the fraction in G_2 increases to as much as 70%. At exposure concentrations in excess of 10 μM, the fraction in G_2 falls off rapidly and is replaced by cells in G_1.

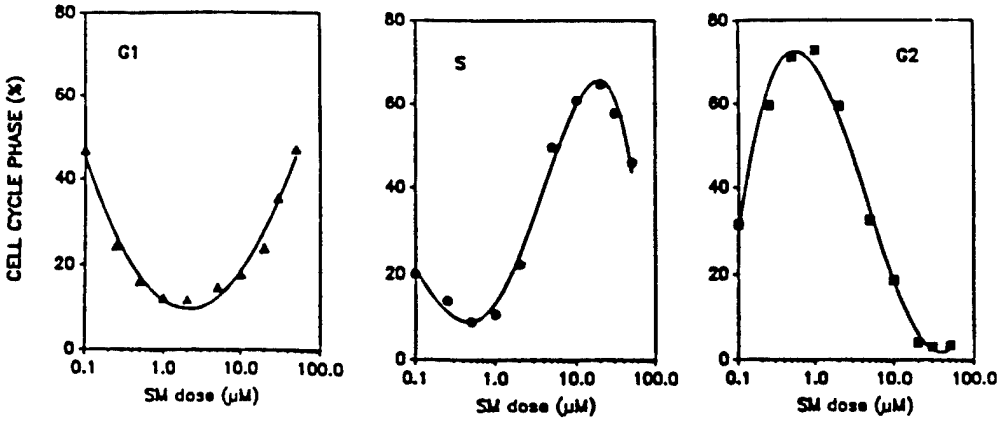

Figure 23. Cell Cycle Distribution Following Exposure to SM. The fraction of cells in G_1, S, and G_2 was determined from cell cycle distributions as shown in Figure 22.

Cell cycle analyses performed during prolonged incubation of cells exposed to low levels of SM demonstrate that progression through S occurs at a slow, dose-dependent rate during the period of growth arrest. Figure 24 (next page) shows cell cycle progression following exposure to 2 μM SM. Control cells shown at the top of this figure are already cycling by day 0 (1 day after plating) and accumulate in G_1 by day 2 as a result of contact inhibition. Exposed cells, on the other hand, proceed slowly through S and accumulate in G_2 by day 2. Eventually, however, cells are released from the G_2/M block and by day 10 show a much more normal distribution. The absence of fragmented DNA throughout suggests that cell death by apoptosis has not occurred.

Release from the G_2/M block coincides with the reinitiation of population growth (increase in TBE cell number) as shown in Figure 15. It also coincides with the recovery of CFA as shown in Figure 19. Thus, an analysis of cell cycle progression after exposure to low levels of SM supports our interpretation of the TBE and CFA data that cells can recover from limited exposure to SM.

Please see next page for Figure 24.

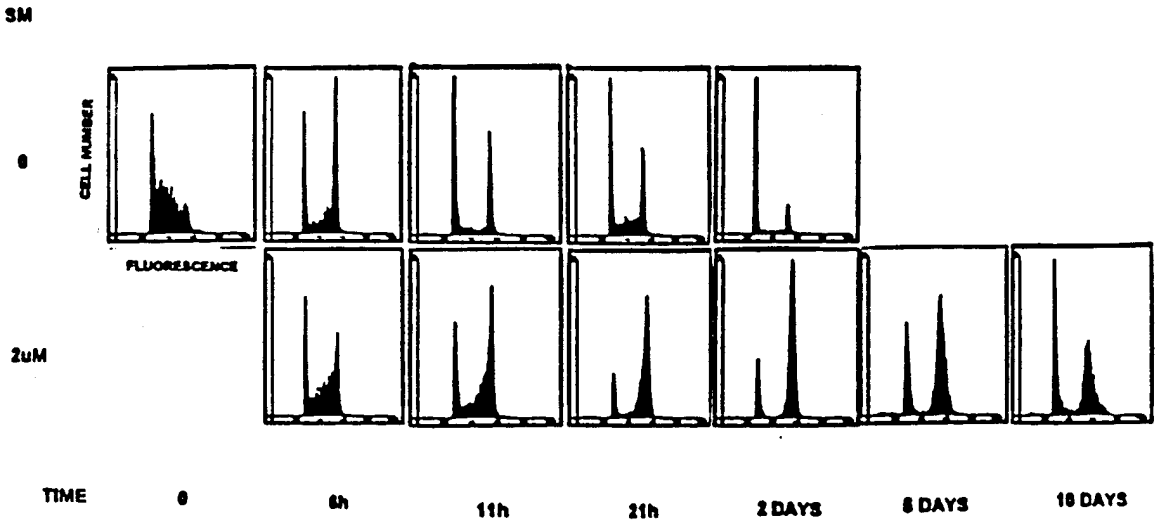

Figure 24. Effect of SM on Cell Cycle Progression. Asynchronized fibroblasts were exposed to 2 μM SM for 1 h at room temperature, the medium was changed, and cells were incubated at 37°C. Cell cycle analysis was performed thereafter as indicated. Top row, control cells; bottom row, exposed cells.

Effects of Cell Cycle Modulation on SM Toxicity

Effects of Ciclopirox

The experiments described above indicate that mammalian cells have some ability to recover from exposure to low concentrations of SM. Experiments described below show that this survival depends on the presence of DNA repair mechanisms. Accordingly, we have explored the hypothesis that modalities which delay cell cycle progression may allow more time for DNA repair and thereby increase survival rate.

As mentioned in the Introduction, one method of arresting cell cycle progression reversibly is through the use of chemicals like ciclopirox olamine (CPX). Figure 25 (next page) illustrates the reversible cell cycle arrest caused by CPX. This figure compares the cell cycle distribution in a population of human fibroblasts held at 8 μM CPX for 11 h with control cells at 6, 11, and 21 h after the addition of CPX. As shown by the analyses in the bottom row of this figure, exposure to CPX results in a G_1/S arrest. However, 10 h after the removal of CPX the cell cycle distribution resembles that of the control population shown in the top row.

Please see next page for Figure 25.

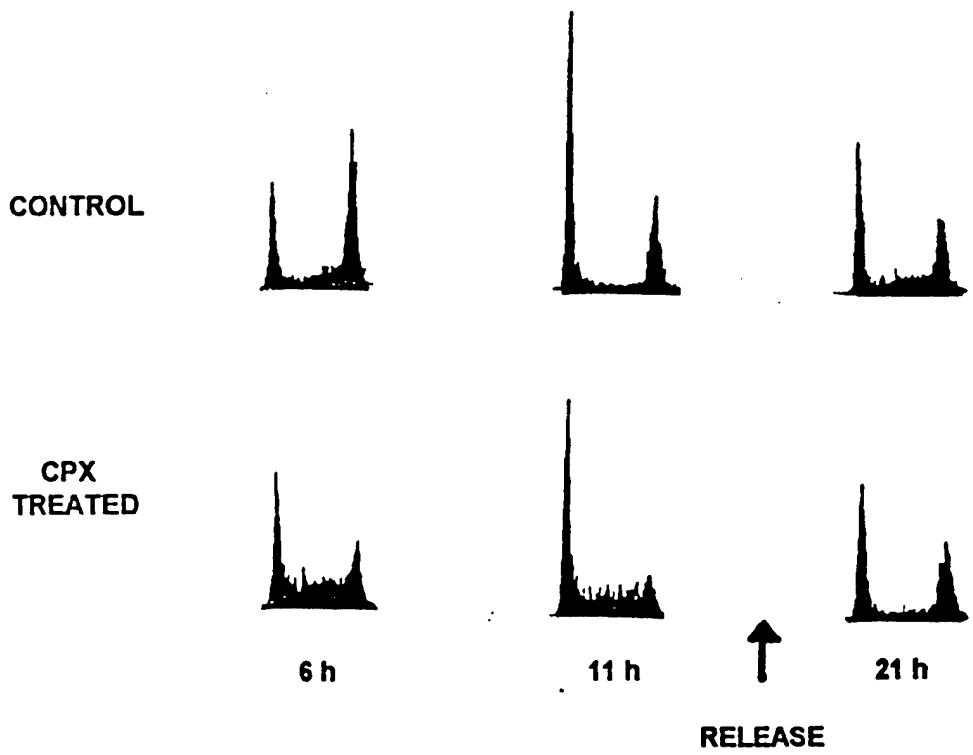

Figure 25. Effect of CPX on Cell Cycle Progression. Human fibroblasts were exposed to 8 μM CPX for 11 h at 37°C; at the end of 11 h, the medium was changed and cells were returned to 37°C for further incubation. Top row, control cells; bottom row, CPX treated.

Figure 26 shows the effect of CPX exposure on cell growth. These data indicate that the cell cycle arrest caused by CPX is eventually overcome and exposed cells return to the same growth rate as control cells.

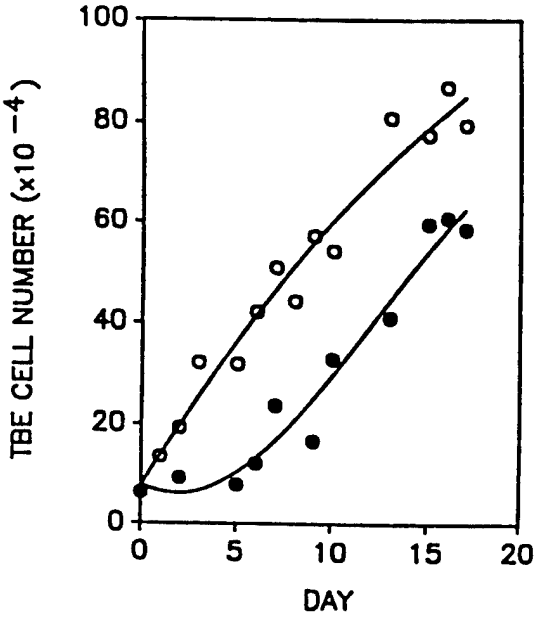

Figure 26. Effect of CPX on Cell Growth. Cells were exposed to 8 μM CPX for 23 h at 37°C; CPX was removed and incubation continued at 37°C. TBE cell number was determined as indicated. Control cells (O); CPX-treated cells (●).

The effect of a CPX arrest on survival after SM exposure was investigated as shown in Figure 27. This figure shows the result of incubating human fibroblasts in the presence of 8 μM CPX before and after exposure to 2 μM SM for 1 h at room temperature. Exposure to SM, in the absence of CPX resulted in a significant decrease in the rate of growth of TBE cells. It is also apparent from this figure that incubation with CPX had practically no effect on the growth of cells exposed to SM.

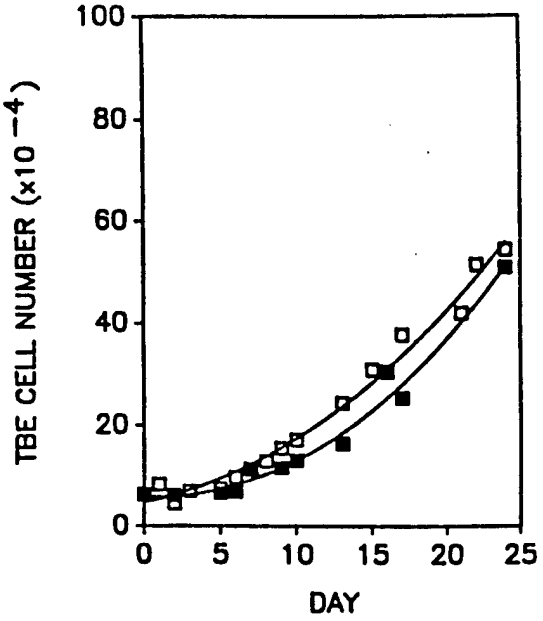

Figure 27. Effect of SM on Human Fibroblasts in the Presence of CPX. Cells were preincubated for 3 h in the presence of 8 μM CPX before exposure to 2 μM SM for 1 h at room temperature. SM-containing medium was replaced with medium containing 8 μM CPX and incubation was continued for an additional 20 h at 37°C. TBE number was determined thereafter as indicated. Control cells were exposed to 2 μM SM in the absence of CPX. Control cells (□): cells exposed to SM in the presence of CPX (■).

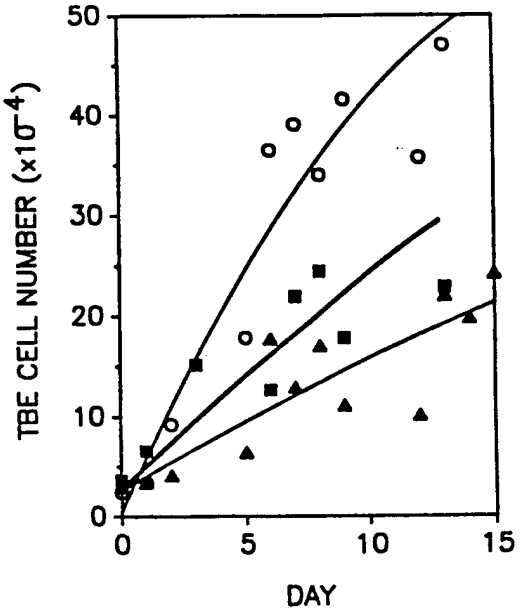

Figure 28. Effect of Hypothermia on Growth of Human Fibroblasts. Cells were plated and grown at 31°C (▲), 33°C (■), or 37°C (O).

These results indicate that CPX is an effective cell cycle arresting agent, but that it does not improve survival after exposure to low concentrations of SM under the conditions tested here.

Effects of Hypothermia

An alternate and probably more benign method of slowing cell growth is by the use of mild hypothermia. Figure 28 shows that human fibroblasts divide and show an increase in number of TBE cells over the temperature range 31°C - 37°C. However, when the temperature is lowered to 28°C, cells remain arrested in G_1 as shown in Figure 29. If the period of hypothermia at 28°C is 24 h or less, and cells are transfered from 28°C to 37°C, they resume growth (data not shown).

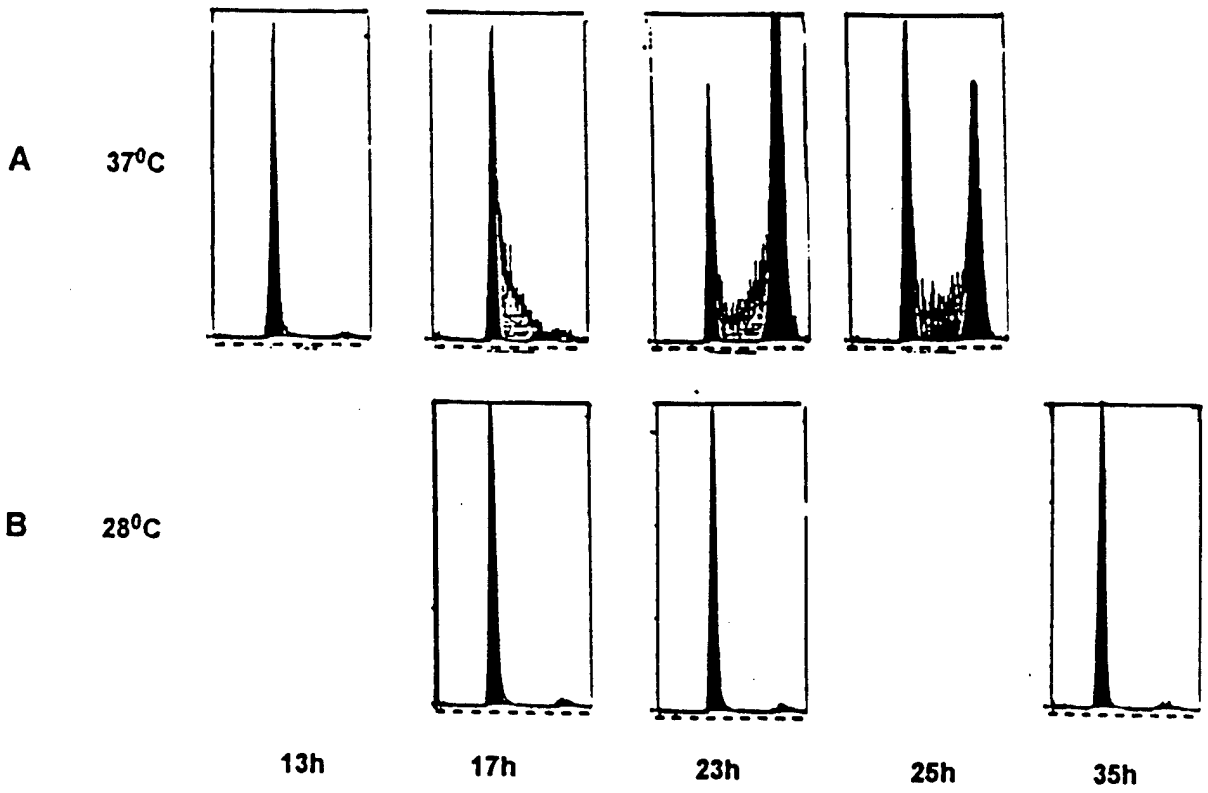

Figure 29. Inhibition of Cell Cycle Progression at 28°C. Fibroblasts were plated at a density of ~2 x 10^4 cells/cm^2 in standard medium and incubated either at 37°C (A) or at 28°C (B); cell cycle analysis was performed at the indicated times.

We next investigated the effect of hypothermia on the growth of human fibroblasts exposed to SM. Figure 30 (next page) shows that cells held at 28°C for 24 h after exposure to 10 μM SM and then returned to 37°C grew at a somewhat faster rate than cells similarly exposed to SM and incubated at 37°C throughout. We conclude that a period of mild hypothermia may increase the survival of cells exposed to low levels of SM, presumably by allowing more time for DNA repair.

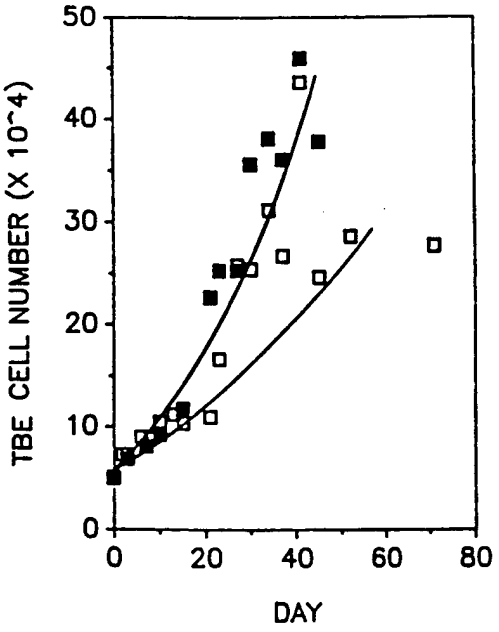

Figure 30. Effect of Hypothermia on SM Toxicity. Fibroblasts were exposed to 10 μM SM for 1 h at room temperature. The medium was changed and cells were incubated either at 37°C (□) throughout the experiment or at 28°C (■) for 1 day before being returned to 37°C.

Either physical or chemical methods of delaying progression through the cell cycle might also interfere with DNA repair. Since we believe that glycosylase action contributes to the repair of SM-induced modifications we have investigated the effects of both temperature and CPX on the activity of human glycosylase assayed with [^{3}H]DMS-modified DNA. The data in Table 4 show that glycosylase does, indeed, retain its activity at 28°C or in the presence of as much as 100 μM CPX. Thus, we believe that glycosylase activity would be unimpaired during reversible cell cycle arrest caused by either hypothermia or CPX.

Table 4. Effect of Hypothermia and Ciclopirox Olamine (CPX) on Human 3-methyladenine DNA Glycosylase Activity

Temperature (°C)	CPX (μM)	Enzyme Activity (cpm released)
37	0	1283
28	0	1153
37	1	1253
37	10	1353
37	100	1283

Effects of DNA Repair on Cell Survival

Effect of Nucleotide Excision Repair

Identification of the DNA repair modalities that protect cells from the toxic effects of SM would assist efforts to improve repair and decrease toxicity. Since Chinese hamster ovary (CHO) cells are available that are deficient in nucleotide excision repair, it is possible to determine the importance of this repair modality in protecting CHO cells from SM. As shown in the left-hand panel of Figure 31, CHO cells lacking the nucleotide excision repair pathway grow as well as competent cells under normal conditions. However, after exposure to 10 μM SM (right-hand panel), repair-deficient cells do not grow at all while competent cells begin to recover after a few days. Thus, it is clear that nucleotide excision repair mechanisms play an important role in protecting cells from SM-inflicted damage.

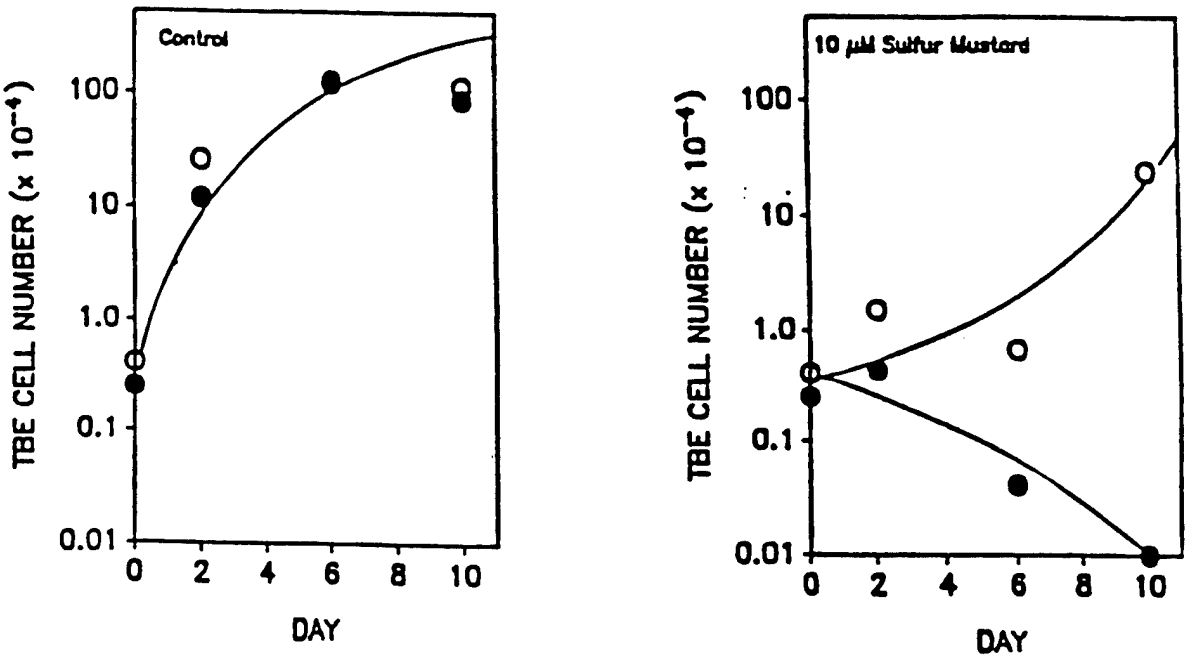

Figure 31. Effect of Nucleotide Excision Repair on Survival of Chinese Hamster Ovary (CHO) Cells Exposed to Sulfur Mustard. Growth, measured by the number of trypan blue excluding cells, is plotted *versus* days of incubation. The left panel shows the growth of wild type (O) and nucleotide excision repair-deficient cells (●) under standard conditions, and the right hand panel shows growth after exposure to 10 μM sulfur mustard.

The data shown in Figure 31 do not indicate which DNA modification or modifications are repaired by this mechanism. Accordingly, we examined the effect of nucleotide excision repair on survival after exposure to hemisulfur mustard which forms the same monoadducts as SM, but does not form the cross-link. As shown in Figure 32 (next page), cells deficient in nucleotide excision repair are also very much more sensitive to hemisulfur mustard. We conclude two things from this experiment: First, monoadduct formation is cytotoxic and second, nucleotide excision repair is effective in protecting cells from the lethal effects of monoadduct formation.

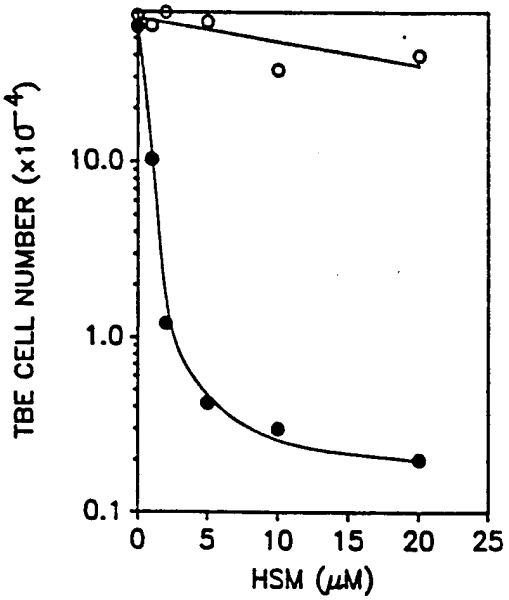

Figure 32. Effect of Nucleotide Excision Repair (NER) on Survival of CHO Cells Exposed to Hemisulfur Mustard. Wild type AA8 (NER-competent, open symbols) and NER-deficient UV41 cells (closed symbols) CHO cells were exposed to different concentrations of HSM for one half hour. Survival was determined by TBE six days later.

Effect of O^6-Alkylguanine-DNA Alkyltransferase

Alkylation of the O^6-position of guanine is known to be a highly toxic event and is a major cause for the cytotoxicity of the chloroethylnitrosoureas, an important class of antitumor agents (8). At the same time, protection against the cytotoxicity that arises from alkylation of the O^6-position of guanine can be provided by the enzymatic action of O^6-alkylguanine-DNA alkyltransferase (8). Consequently, we wondered whether O^6-alkylguanine-DNA alkyltransferase would protect mammalian cells from the toxicity of SM.

To answer this question, we obtained CHO cells that had been transfected with human O^6-alkylguanine-DNA alkyltransferase (AT) from our colleague Dr. Edward Bresnick (42). Since CHO cells are normally deficient in AT activity, a side by side comparison of the cytotoxicity of SM for the control *versus* AT transfected cells would reveal the importance of alkyltransferase activity.

As shown in Figure 33 (next page), the cytotoxicity of 2 μM or 50 μM SM is the same towards both cell lines. Positive controls, not shown here, demonstrated a marked difference in the cytotoxicity of the chloroethylnitrosoureas for these two cell lines in agreement with the results of Wu et al (42). We conclude that O^6-alkylguanine-DNA alkyltransferase is not an important factor in preventing SM toxicity.

However, this does not rule out O^6-alkylation of guanine as a cytotoxic action of SM because O^6-alkylguanine-DNA alkyltransferase may not be effective in removing the bulky hydroxyethylthioethyl adduct that would be formed by SM (49). Nucleotide excision repair, on the other hand, is known to act on bulkier groups attached to the O^6-position of guanine and might repair O^6-hydroxyethylthioethyl guanine.

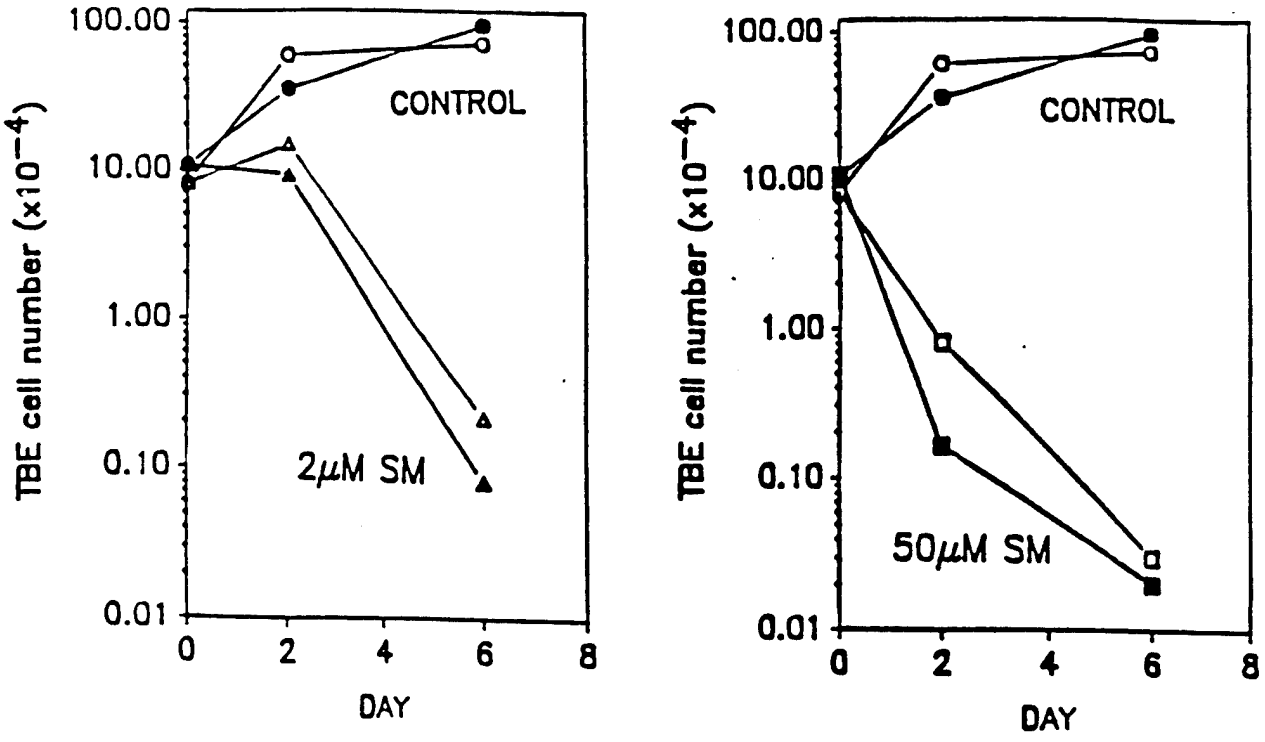

Figure 33. Lack of Effect of O^6-alkylguanine-DNA Alkyltransferase on Survival of CHO Cells Exposed to SM. UV41 CHO cells (open symbols) and UV41 CHO cells transfected with a plasmid expressing human O^6-alkylguanine-DNA alkyltransferase (closed symbols) were exposed to 2 μM (triangles, left-hand panel) or 50 μM (squares, right-hand panel) SM. Control cells exposed to 0 μM SM (circles) are shown at the top of each panel. Survival was determined by the TBE exclusion assay two and six days after exposure.

We conclude from this that efforts to increase levels of O^6-alkylguanine-DNA alkyltransferase would not be helpful in relieving SM toxicity. However, if SM alkylates the O^6-position of guanine, NER repair may be effective in lessening toxicity resulting from this DNA modification.

DISCUSSION

The results presented above show that DNA repair plays an important role in protecting mammalian cells from SM toxicity. The absence of nucleotide excision repair, in particular, is accompanied by a major increase in the sensitivity of CHO cells to SM. Furthermore, it is probable that base excision repair also plays a protective role against SM toxicity since mammalian glycosylase recognizes and releases both 3-hydroxyethylthioethyl adenine (HETEA) and 7-hydroxyethylthioethyl guanine (HETEG) from SM-modified DNA.

Studies of antitumor agents suggest that a normal cellular defense against DNA damage is to delay cell cycle progression to allow more time for DNA repair. We believe that this defensive mechanism can be enhanced by modalities which cause a reversible cell cycle arrest. Indeed, a brief period of hypothermia has been shown to decrease the cytotoxicity of SM for fibroblasts.

It is not yet known, however, which DNA lesions are repaired during the period of hypothermia or what repair modalities are active. Answers to these questions can presumably be obtained by monitoring levels of DNA damage during recovery and by investigating DNA repair in cell lines for which a protective effect has been established.

The following sections discuss the nature and quantification of SM-induced DNA damage, experiments that relate DNA repair to SM toxicity, and the role of cell cycle progression in SM toxicity.

Sulfur Mustard-induced DNA Modifications

Alkylation of the O^6-position of Guanine by SM

Although the major sites of DNA alkylation are the 7 position of guanine and the 3 position of adenine, minor sites of DNA modification have been shown to be important for the cytotoxic action of other DNA modifying agents. In particular, alkylation of the O^6-position of guanine is often a critical event.

Accordingly, both our laboratory and that of Dr. H.P. Benschop have investigated the question of O^6-guanine alkylation by SM. Both laboratories have been successful in synthesizing O^6-hydroxyethylthioethyl guanine and O^6-hydroxyethylthioethyl deoxyguanosine and are in agreement as to the ultraviolet and mass spectrometric characterization of these marker compounds (see Results section and reference 16). However, neither laboratory has succeeded in establishing the presence of this adduct in DNA.

SM does react with deoxyguanosine to produce small amounts of O^6-hydroxyethylthioethyl deoxyguanosine as shown in Figure 4. It seems probable that this reaction also occurs in DNA, but the adduct decomposes under standard DNA hydrolysis conditions as shown in Figure 5. Recently, we have shown that O^6-hydroxyethylthioethyl deoxyguanosine can be recovered in approximately 50% yield after incubation under the conditions that we use for enzymatic digestion in the ^{32}P-postlabeling analysis (12°C and pH 7.5). Consequently, it will be possible to reexamine this question with the higher specific activity [^{14}C]SM now available.

^{32}P-Postlabeling Analysis of SM-induced DNA Modifications

Although minor sites of alkylation may have an important biological significance, 7-hydroxyethylthioethyl guanine is formed in the greatest amounts by the reaction of SM with DNA. Accordingly, methods of measuring this adduct provide useful information on exposure. Although earlier attempts to apply the ^{32}P-postlabeling method to detection of the 7-alkylguanines formed by chemotherapeutic alkylating agents have been unsuccessful, we have overcome this problem by the use of low temperature digestion as described previously (42).

The key to adapting this previously-reported *in vitro* method to *in vivo* analyses was in modifying the DNA isolation step. The use of salt precipitation and the avoidance of organic solvents allowed us to isolate DNA from cultured cells in a manner that did not affect adduct levels.

The level of DNA modification reported here, one HETEpdG/10^6 nucleotides in fibroblasts exposed to 2.3 μM SM, can be compared with values reported previously for *in vitro* exposure of white blood cells. Using a less sensitive fluorometric method of detection, we found that exposure of whole blood to 131 μM SM resulted in 157 HETEpdG/10^6 nucleotides in white blood cell DNA (13). Van der Schans and colleagues, using a much more sensitive immunochemical method of detection, reported that exposure of whole blood to 2 μM SM resulted in 2.5 HETEpdG/10^6 nucleotides (12). Assuming a linear relationship between HETEpdG level and SM concentration, both of these results would predict that one HETEpdG/10^6 nucleotides would be produced in white blood cells by 0.8 μM SM. Although the conditions of exposure may have varied somewhat among these different experiments, this would suggest that the level of DNA modification at a given SM concentration is slightly lower in fibroblasts grown in cell culture than in white blood cells.

As shown by the data in Fig. 13, growth of fibroblasts is only somewhat retarded by 2 μM SM. Thus, both the immunochemical and ^{32}P-postlabeling technique have the sensitivity necessary to detect DNA modifications in the toxic range. Although both methods have been applied to the most prevalent DNA modification, HETEG, it can be assumed that levels of other DNA adducts parallel HETEG in amounts. Therefore the ability to measure this adduct at growth-inhibiting concentrations of SM should provide a valuable tool for investigating exposure.

We would like to add one caveat about the storage of DNA samples prior to analysis by the ^{32}P-postlabeling technique. Although duplicate determinations on frozen samples have been reproducible over a period of a month, we have found that HETEpdG levels fall during longer periods of storage. Since this decrease seems to exceed the rate of loss of HETEG by spontaneous depurination, it may represent a change in DNA structure which inhibits the digestion that is necessary for ^{32}P-postlabeling analysis. These results, which have not been fully quantitated, suggest that DNA analysis should follow DNA isolation promptly.

Repair of SM-induced DNA Modifications

The biochemical experiments shown in Figures 10 - 14 strongly suggest that base excision repair initiated by glycosylase action plays an important role in protecting cells from SM toxicity. Bacterial and human glycosylases both recognize and release HETEG and HETEA at rates which compare favorably with their activity towards methylated bases. Neither enzyme releases the cross-link, di-(2-guanin-7-yl-ethyl)sulfide, which is significant because the increased toxicity of bifunctional sulfur mustards over one-armed mustards has been attributed to their ability to form this cross-link (3). However, the results reported here do not eliminate the possibility that glycosylase acts to "unhook" a cross-link *in vivo* as suggested by Reid and Walker (50). Other repair modalities including nucleotide excision repair and recombination repair may also act on the cross-link.

Nucleotide excision repair is clearly important in preventing SM cytotoxicity as shown by the survival data in Figure 31. Accordingly, methods of increasing the efficiency of this repair mechanism should decrease SM toxicity.

SM-induced Cytotoxicity

Most of the studies on SM cytotoxicity reported above have been performed on normal human fibroblasts grown in cell culture. These cells are favorable for study because they appear to retain normal controls on cell cycle progression. Thus, it is possible to test our hypothesis that slowing the cell cycle may allow more time for DNA repair and diminish SM toxicity. However, the importance of nucleotide excision repair has been tested on CHO cells which have the advantage of being characterized for competency in this repair modality. Comparison studies have also been performed on cultured NM-1 keratinocytes.

Figures 15 and 16 show that micromolar concentrations of SM cause a reversible arrest in population growth as determined by the TBE assay. Fibroblast appearance changes after exposure and cells become large and somewhat distorted, a condition often referred to as "unbalanced growth". However, the percentage of trypan blue non-excluding cells remained low and did not increase with SM concentrations up to 20 μM. Furthermore, the cells' appearance returned to normal when they began to divide again. We take this as evidence that human fibroblasts are able to recover from exposure to low levels of SM and we believe the recovery is related to their ability to undergo a cell cycle arrest while DNA damage is repaired.

Cell cycle analyses performed at different time points during prolonged post-exposure incubation support our interpretation that cells can recover from low exposures to SM. Exposed cells progress slowly through S and accumulate in G_2. Release from the G_2/M block coincides with the reinitiation of population growth as measured by TBE. It also coincides with the recovery of CFA, and we believe that all of these events may coincide with completion of DNA repair.

Hypothermia produces a reversible cell cycle arrest in cultured human fibroblasts and appears to facilitate the return of normal cell growth in SM-exposed cells. Accordingly, we believe that the use of mild hypothermia offers some promise as a modality for decreasing SM toxicity.

CONCLUSIONS

The data reported above provide support for the following hypotheses: 1. SM toxicity is initiated by DNA modification. 2. DNA repair decreases SM toxicity. 3. Modalities which slow cell cycle progression decrease toxicity, probably by allowing more time for DNA repair.

Exposure of cultured human fibroblasts to micromolar concentrations of SM causes a dose-dependent arrest in the growth of trypan blue excluding (TBE) cells. During the period of growth arrest, cells increase in size and appear abnormal, but return to a normal appearance with the reinitiation of cell division. During the period of time when cells are not dividing, they are arrested in the G_2 phase of the cell cycle; increase in the number of TBE cells and in the colony forming ability occur when the G_2/M block is released. We believe that the G_2/M block may be an adaptive response allowing cells to repair DNA damage.

Studies of Chinese hamster ovary (CHO) cells show that nucleotide excision repair provides important protection against SM cytotoxicity. Glycosylase action also apparently plays an important role in protecting cells from SM toxicity. Both bacterial and human glycosylase release 7-hydroxyethylthioethyl guanine (HETEG) and 3-hydroxyethylthioethyl adenine (HETEA) from DNA that has been alkylated by SM.

We believe that modalities which retard cell cycle progression may allow more time for DNA repair and decrease SM cytotoxicity. The chemical agent, ciclopirox, results in a G_1 arrest but does not seem to decrease SM toxicity. On the other hand, a brief period of hypothermia which apparently causes a more general cell cycle arrest, does result in an improvement in the growth of fibroblasts subsequently incubated at 37°C.

Finally, we have adapted the ^{32}P-postlabeling technique to the detection of 7-hydroxyethylthioethyl guanine in fibroblasts exposed to low micromolar levels of SM in cell culture. We have found that one HETEG per 10^6 nucleotides is produced at a SM concentration of 2.3 μM, a concentration that is minimally toxic. Accordingly, this analytical method should prove useful in monitoring exposure.

REFERENCE LIST

1. Willems, J. L. Clinical Management of Mustard Gas Casualties. Annales Medicinae Militaris Belgicae, *3*, S1-S61, 1989.

2. IARC Monographs on the evaluation of carcinogenic risks to humans: Overall evaluations of carcinogenicity: An updating of IARC Monographs Volumes 1 to 42. International Agency for Research on Cancer, Lyon. Suppl. *7*, 259-260, 1987.

3. Papirmeister, B., Feister, A. J., Robinson, S. I. and Ford, R. D. Medical Defense Against Mustard Gas: Toxic Mechanisms and Pharmacological Implications. CRC Press, 1991.

4. Goodman, L. S., Wintrobe, M. M., Dameshek, W., Goodman, M. J., Gilman, A. (Major) and McLennan, M. T. Nitrogen Mustard Therapy. J. Am. Med. Assoc. *132*, 126-132, 1946.

5. Hemminki, K. and Ludlum, D. B. Covalent modification of DNA by antineoplastic agents. J. Natl. Cancer Inst. *73*, 1021-1028, 1984.

6. Colvin, M. Alkylating Agents and Platinum Antitumor Compounds. *In:* J. F. Holland, E. Frei, III, R. C. Bast, Jr., D. W. Kufe, D. L. Morton, R. R. Weichselbaum (eds.), Cancer Medicine, 3rd Edition, Vol. 1, pp. 733-754, Lea & Febiger, Philadelphia/London, 1993.

7. Chabner, B. A., Allegra, C. J., Curt, G. A. and Calabresi, P. Antineoplastic agents. In: *Goodman and Gilman's The Pharmacological Basis of Therapeutics*, 9th Edition, pp. 1233-1287, New York, McGraw-Hill, 1996.

8. Ludlum, D. B. The chloroethylnitrosoureas: Sensitivity and resistance to cancer chemotherapy at the molecular level. Cancer Investigation, in press.

9. Rydberg, B. and Lindahl, T. Nonenzymatic methylation of DNA by the intracellular methyl group donor S-adenosyl-L-methionine is a potentially mutagenic reaction. EMBO J. *1*, 211-216, 1982.

10. Barrows, L. R. and Magee, P. N. Nonenzymatic methylation of DNA by S-adenosylmethionine *in vitro*. Carcinogenesis *3*, 349-351, 1982.

11. Brookes, P., and Lawley, P. D. The reaction of mustard gas with nucleic acids *in vitro* and *in vivo*. Biochem. J. *77*, 478-484, 1960.

12. van der Schans, G. P., Scheffer, A. G., Mars-Groenendijk, R. H., Fidder, A., Benschop, H. P. and Baan, R. A. Immunochemical detection of adducts of sulfur mustard to DNA of calf thymus and human white blood cells. Chem. Res. Toxicol. *7*, 408-413, 1994.

13. Ludlum, D. B., Austin-Ritchie, P., Hagopian, L., Niu, T.-q. and Yu, D. Detection of sulfur mustard-induced DNA modifications. Chem.-Biol. Interactions *91*, 39-49, 1994.

14. Ludlum, D. B., Kent, S. and Mehta, J. R. Formation of O^6-ethylthioethylguanine in DNA by reaction with the sulfur mustard, chloroethyl ethyl sulfide, and its apparent lack of repair by O^6-alkylguanine-DNA alkyltransferase. Carcinogenesis *7*, 1203-1206, 1986.

15. Ludlum, D. B. Protection against the acute and delayed toxicity of mustards and mustard-like compounds, Annual/Final Report, Contract No. DAMD17-82-C-2203, U.S. Army Medical Research and Development Command, 1987.

16. Fidder, A., Moes, G. W. H., Scheffer, A. G., van der Schans, G. P., Baan, R. A., de Jong, L. P. A., and Benschop, H. P. Synthesis, characterization and quantitation of the major adducts formed between sulfur mustard and DNA of calf thymus and human blood. Chem. Res. Toxicol. *7*, 199-204, 1994.

17. Papirmeister, B. and Davison, C. L. Elimination of sulfur mustard-induced products from DNA of *Escherichia coli*. Biochem. and Biophys. Res. Comm., *17*, 608-617, 1964.

18. Lawley, P. D. and Brookes, P. Molecular mechanism of the cytotoxic action of difunctional alkylating agents and of resistance to this action. Nature *206*, 480-483, 1965.

19. Venitt, S. Interstrand cross-links in the DNA of *E. coli* B/r and Bs-1 and their removal by the resistant strain. Biochem. Biophys. Res. Comm. *31*, 355-360, 1968.

20. Crathorn, A. R. and Roberts, J. J. Mechanism of the cytotoxic action of alkylating agents in mammalian cells and evidence for the removal of alkylated groups from deoxynucleic acid. Nature *211*, 150-153, 1966.

21. Reid, B. D. and Walker, I. D. The response of mammalian cells to alkylating agents II. On the mechanism of the removal of sulfur-mustard-induced cross-links. Biochim. Biophys. Acta *179*, 179-188, 1969.

22. Mol, M. A. E., van der Schans, G. P. and Lohman, P. H. M. Quantification of sulfur mustard-induced DNA interstrand cross-links and single-strand breaks in cultured human epidermal keratinocytes. Mutat. Res. *294*, 235-245, 1993.

23. Papirmeister, B., Gross, C. L., Meier, H. L., Petrali, J. P. and Johnson, J. B. Molecular basis for mustard-induced vesication. Fundam. and Appl. Toxicol. *5*, S134-S149, 1985.

24. Habraken, Y. and Ludlum, D. B. Release of chloroethyl ethyl sulfide-modified DNA bases by bacterial 3-methyladenine-DNA glycosylases I and II. Carcinogenesis *10*, 489-492, 1989.

25. Nelson, W. G. and Kastan, M. B. DNA strand breaks: the DNA template alterations that trigger p53-dependent DNA damage response pathways. Mol Cell Biol. *14*, 1815-1823, 1994.

26. Murray, A. W. Coordinating cell cycle events. Cold Spring Harbor Symposia on Quantitative Biology 56, 399-408, 1991.

27. Murray, A. W. Creative blocks: cell-cycle checkpoints and feedback controls. Nature *359*, 599-604, 1992.

28. O'Connor, P. M., Ferris, D. K., White, G. A., Pines, J., Hunter, T., Longo, D. L. and Kohn, K. W. Relationships between cdc2 kinase, DNA cross-linking, and cell cycle perturbations induced by nitrogen mustard. Cell Growth & Differentiation *3*, 43-52, 1992.

29. O'Connor, P. M., Ferris, D. K., Hoffmann, I., Jackman, J., Draetta, G. and Kohn, K. W. Role of the cdc25C phosphatase in G2 arrest induced by nitrogen mustard. Proc. Natl. Acad. Sci. USA *91*, 9480-9484, 1994.

30. O'Connor, P. M., Ferris, D. K., Pagano, M., Draetta, G., Pines, J., Hunter, T., Longo, D. L. and Kohn, K. W. G2 delay induced by nitrogen mustard in human cells affects cyclin A/cdk2 and cyclin B1/cdc2-kinase complexes differently. J. Biol. Chem. *268*, 8298-8308, 1993.

31. Hoffman, B. D., Hanauske-Abel, H. M., Flint, A., and Lalande, M. A new class of reversible cell cycle inhibitors. Cytometry *12*, 26-32, 1991.

32. Levenson, V., and Hamlin, J. L. A general protocol for evaluating the specific effects of DNA replication inhibitors. Nucleic Acids Res. *21*, 3997-4004, 1993.

33. Whitmore, G. F., and Gulyas, S. Studies on recovery processes in mouse L cells. Natl. Cancer Inst. Monogr. No. 24, pp. 141-156, 1965.

34. Winans, L. F., Dewey, W. C., and Dettor, C. M. Repair of sublethal and potentially lethal x-ray damage in synchronous Chinese hamster cells. Radiat. Res. *52*, 333-351, 1972.

35. Robins, H. I., Hugander, A., and Cohen, J. D. Whole body hyperthermia in the treatment of neoplastic disease. Radiol. Clin. North Am. *27*, 603-10, 1989.

36. Tsou, K. C., Su, H. C. F., Segebarth, C., and Mirarchi, U., Synthesis of possible cancer chemotherapeutic compounds based on enzyme approach I. Hemisulfur mustard and its esters. J. Org. Chem. *26*, 4987-4990, 1961.

37. Ludlum, D. B. Protection Against the Acute and Delayed Toxicities of Mustards and Mustard-Like Compounds, Final Report, 24 February 1993, Contract No. DAMD17-89-C-9011, U.S. Army Medical Research and Development Command, 1993.

38. Gambino, J., Yang, T.-F., and Wright, G. E. Identification of purine deoxyriboside anomers by two dimensional NOESY NMR. Tetrahedron, submitted manuscript, 1994.

39. Matijasevic. Z. M., Bodell, W. J., and Ludlum, D. B. 3-Methyladenine DNA glycosylase activity in a glial cell line sensitive to the haloethylnitrosoureas in comparison with a resistant cell line. Cancer Res. *51*, 1568-1570, 1991.

40. Foote, R. S., and Mitra, S. Lack of induction of O6-methylguanine-DNA methyltransferase in mammalian cells treated with N-methyl-N'-nitro-N-nitrosoguanidine. Carcinogenesis. *5*, 277-81 (1984).

41. Wu, Z., Chan, C.-L., Eastman, A. and Bresnick, E. Expression of human O^6-methylguanine-DNA methyltransferase in Chinese hamster ovary cell and restoration of cellular resistance to certain N-nitrosourea compounds. Molecular Carcinogenesis 4, 482-488, 1991.

42. Yu, D., Niu, T.-q., Austin-Ritchie, P. and Ludlum, D. B. A ^{32}P-postlabeling method for detecting unstable N-7 substituted deoxyguanosine adducts in DNA. Proc. Natl. Acad. Sci. USA *91*, 7232-7236, 1994.

43. Shields, P. G., Povey, A. C., Wilson, V. L., Weston, A. and Harris, C. C. Combined high-performance liquid chromatography/^{32}P-postlabeling assay of N7-methyldeoxyguanosine. Cancer Res. *50*, 6580-6584, 1990.

44. Mustonen, R., Försti, A., Hietanen, P. and Hemminki, K. Measurement by ^{32}P-postlabelling of 7-methylguanine levels in white blood cell DNA of healthy individuals and cancer patients treated with dacarbazine and procarbazine. Human data and method development for 7-alkylguanines. Carcinogenesis *12*, 1423-1431, 1991.

45. Miller, S. A., Dykes, D. D. and Polesky, H. F. A simple salting out procedure for extracting DNA from human nucleated cells. Nucleic Acids Res. *16*, 1215, 1988.

46. Nakabeppu, Y., Kondo, H. and Sekiguchi, M. Cloning and characterization of the alkA gene of Escherichia coli that encodes 3-methyladenine DNA glycosylase II. J. Biol. Chem. *259*, 13723-13729, 1984.

47. Samson, L., Derfler, B., Boosalis, M., Call, K. Cloning and characterization of a 3-methyladenine DNA glycosylase cDNA from human cells whose gene maps to chromosome 16. Proc. Natl. Acad. Sci. USA *88*, 9127-9131, 1991.

48. Gupta, R. C. and Randerath, K. Analysis of DNA adducts by ^{32}P labeling and thin layer chromatography, In: E.C. Freidberg and P.C. Hanawalt (Eds.), *DNA Repair. A Laboratory Manual of Research Procedures*, Vol. 3, Marcel Dekker, Inc., New York and Basel, 1988, pp. 399-418.

49. Pegg, A. E. Mammalian O^6-alkylguanine-DNA alkyltransferase: Regulation and importance in response to alkylating carcinogenic and therapeutic agents. Cancer Res. *50*, 6119-6129, 1990.

50. Reid, B. D., and Walker, I. D. The response of mammalian cells to alkylating agents II. On the mechanism of the removal of sulfur mustard-induced cross-links. Biochim. Biophys. Acta *179*, 179-188, 1969.

APPENDIX

List of Publications Supported by this Contract:

1. Yu, D., Niu, T.-q., Austin-Ritchie, P., and Ludlum, D. B. A ^{32}P-postlabeling method for detecting unstable N-7 substituted deoxyguanosine adducts in DNA. Proc. Natl. Acad. Sci. USA *91*, 7232-7236, 1994.

2. Ludlum, D. B., Austin-Ritchie, P., Hagopian, M., Niu, T.-q., and Yu, D. Detection of sulfur mustard-induced DNA modifications. Chem.-Biol. Interactions *91*, 39-49, 1994.

3. Niu, T.-q., Matijasevic, Z., Austin-Ritchie, P., and Ludlum, D. B. A ^{32}P-postlabeling method for the detection of adducts in the DNA of human fibroblasts exposed to sulfur mustard. Chem.-Biol. Interactions, in press.

4. Matijasevic, Z., Niu, T.-q., Austin-Ritchie, P., and Ludlum, D. B. Release of the sulfur mustard DNA adduct, 7-hydroxyethylthioethylguanine, by 3-methyladenine DNA glycosylase II. Submitted to Carcinogenesis.

5. Matijasevic, Z., Stering, A., Ludlum, D. B. Toxicity of sulfur mustard for human fibroblasts grown in cell culture. Submitted to the Journal of the American College of Toxicology.

6. Yu, D., Niu, T.-q., Austin-Ritchie, P., and Ludlum, D. B. ^{32}P-Postlabeling of unstable deoxyguanosine adducts in DNA. Proc. Am. Assoc. for Cancer Res. *35*, 99, 1994.

7. Matijasevic, Z., Stering, A., Austin-Ritchie, P. and Ludlum, D.B. Effect of sulphur mustard on growth and cell cycle progression in human fibroblasts. Proc. Am. Assoc. for Cancer Res. *36*, 157, 1995.

8. Matijasevic, Z., Stering, A., Niu, T-q., Austin-Ritchie, P. and Ludlum, D.B. Release of sulfur mustard-modified bases from DNA by 3-methyladenine DNA glycosylase II. Proc. Am. Assoc. for Cancer Res. *37*, 123, 1996.

List of Personnel Receiving Contract Support:

David B. Ludlum, Ph.D., M.D.	Principal Investigator
Zdenka Matijasevic, Ph.D.	Assistant Professor
Dong Yu, Ph.D.	Research Associate
Tian-qi Niu, Ph.D.	Research Associate
Paula Austin-Ritchie	Professional Technician
Christopher Tipper	Laboratory Technician
Allen Stering	Laboratory Technician